SENSOR FOR TURBINE ENGINE ATURE FROM 600 TO 1900°C

FINAL REPORT
NTRACT NAS3-25451
POSAL NO. ~~91-3-38SA~~
EASE DATE ~~8/13/93~~

by
labrese, P. Kaplin and M. Finney

BUFFALO CORPORATION
300 Walden Avenue
falo, New York 14225

86 Phase II

December 1990

Prepared for

R. J. Baumbick

AUTICS AND SPACE ADMINISTRA
vis Research Center
00 Brookpark Road
eveland, OH 44135

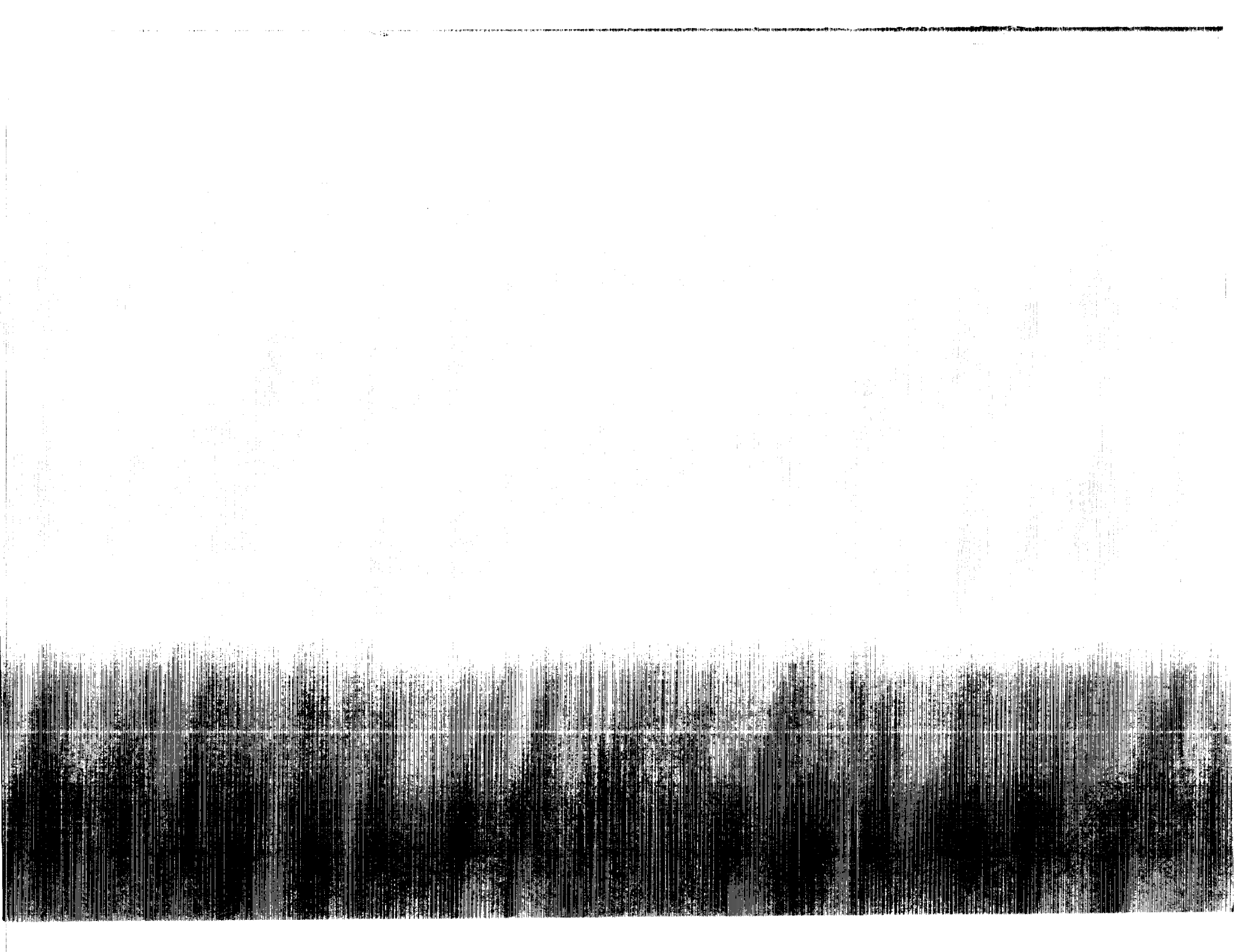

NASA
National Aeronautics and Space Administration

Report Documentation Page

1. Report No.	2. Government Accession No.	3. Recipient's Catalog No.
CR 187048		

4. Title and Subtitle
Fiber Optic Sensor for Turbine Engine Gas Temperature from 600 to 1900°C

5. Report Date
December, 1990

6. Performing Organization Code

7. Author(s)
G. Tregay, P. Calabrese, P. Kaplin and M. Finney

8. Performing Organization Report No.
R & D 1011.02

10. Work Unit No.

9. Performing Organization Name and Address
Conax Buffalo Corporation
2300 Walden Avenue
Buffalo, NY 14225

11. Contract or Grant No.
NAS3-25451

13. Type of Report and Period Covered
Final
May, 1988 to Sept., 1990

12. Sponsoring Agency Name and Address
National Aeronautics and Space Administration
Lewis Research Center
Cleveland, Ohio 44135-3191

14. Sponsoring Agency Code

15. Supplementary Notes

16. Abstract A fiber optic sensor has successfully measured gas temperature in an aircraft turbine engine. The four probe system with an optical cable harness was tested as functional replacement for four thermocouples used to measure turbine discharge temperature on a F404 engine. The duration of the engine test exceeded 50 hours. The sensing element was tested in a propane flame to 1931°C at low velocity, and up to 1500°C at Mach 0.37. An optical cable harness passed environmental tests at -48 to 260°C. All the necessary signal conditioning to accept an optical signal and produce a digital value of probe temperature from 600 to 1900°C was packaged in a 220 x 120 x 85 mm enclosure. The signal processor operated over the -55 to 75°C environment associated with electronic controls. Probe, cable and processor passed sinusoidal vibration tests. The signal processing used a ratio of intensity in two spectral bands and additional compensation to accurately determine temperature in spite of signal perturbation introduced by cables, connectors, and environmental factors.

17. Key Words (Suggested by Author(s)) Gas Turbine Sensor, Fiber Optic Sensor, Gas Turbine Engine, Gas Turbine Instrumentation.

18. Distribution Statement

19. Security Classif. (of this report)	20. Security Classif. (of this page)	21. No of pages	22. Price*
Unclassified	Unclassified	73	

*For sale by the National Technical Information Service, Springfield, Virginia 22161

FORWARD

Many individuals took time to discuss temperature measurement in turbine engines with the investigators and this help contributed to the success of this program. The testing of the sensor at turbine engine conditions requires facilities that are not available at Conax Buffalo Corporation. General Electric Aircraft Engines and Pratt & Whitney provided test facilities and test cell operation to allow the probes to be evaluated under actual turbine conditions. Joe Abraham, GEAE, and Dick Strange, P&W, were especially instrumental in making arrangements and coordinating test cell activity.

TABLE OF CONTENTS

ILLUSTRATIONS

LIST OF TABLES

1.0 SUMMARY

An optical sensor system has been constructed to measure gas temperature in gas turbine engines from 600 to 1900°C (1112 to 3452°F). The sensing element uses radiation from a thermally emissive insert in a sapphire rod. The sapphire rod acts as both a lightguide and shroud. The small diameter provides a faster response time compared to conventional probes with shrouds. The radiation from the sapphire lightguide is transmitted through a flexible optical fiber to a signal processor contained on a 109 x 210 mm (4.30 x 8.26 in) circuit board. The temperature is determined from the ratio of optical intensity in two spectral bands. The ratio technique provides for an accurate measurement by compensating for the transmission variability in the optical components. The effects of environmental temperature on the photodetectors and signal amplifiers is also accounted for in the signal processing. Built-in-test functions include detection of low signal level and when the ratio is outside the calibration range. Two complete sensor systems were delivered at the completion of the contract.

The suitability of the sensor system for on-engine operation was demonstrated in a series of environmental temperature and vibration tests. The sensing element passed flame tests of 1921°C (3489°F) at low velocity and 1500°C (2732°F) at Mach .37. Vibrational testing of the probe assemblies was conducted at frequencies from 10 to 2000 Hz with accelerations up to 20g's. The optical connector at the probe was tested from -48 to 300°C (-54 to 572°F) and the cable assembly tested from -55 to 200°C (-67 to 392°F). Vibration of the optical cable at a 30 Hz resonance for 2 hours did not decrease transmission. The signal processor was operated over a temperature range of -55 to 75°C (-67 to 167°F) and passed a 5g vibration test with the vibration normal to the plane of the circuit board.

A four-probe system with optical cable harness was tested as a functional replacement for the four thermocouple probes used to measure gas temperature between the turbine and the afterburner on a General Electric Aircraft Engines F404 engine. The duration of the engine test exceeded 50 hours and 1000 thermal cycles. The average of the four optical probes located on the upper half of the engine agreed with the average of the four thermocouples on the lower half of the engine. The probes with insert sensing elements were still functional at the end of the test. Areas of improvement for durability and accuracy were identified as a result of these tests.

2. BACKGROUND

Conventional gas temperatures sensors for turbine engines have a limit of about 1100°C (2012°F) (ref. 1) whereas combustor exit engine temperatures have progressed steadily upward and now exceed 1350°C (2462°F) (ref.2). Engine performance has been further enhanced by electronic engine control (ref. 3), however, the immunity of the control system and its sensors to electromagnetic effects must be increased (ref. 4).

The need to improve sensor performance (and potentially reduce weight) has led to the investigation of fiber optics for turbine engine control. This effort encompasses temperature as well as other types of sensors and has been funded under the Fiber Optic Control System Integration (FOCSI) Program (refs. 5-9) and other parallel activity (refs. 10,11).

Fiber optic temperature sensing offers potential advantages for both measurement at higher temperatures and a lower weight sensor harness. Optical quality sapphire is an attractive material for the lightguide because of its high melting point, 2045°C (3713°F), and chemical inertness at high temperature. The basic concept of using a coated sapphire lightguide for temperature measurement was proposed in 1971 (ref. 12). This sensor determines the temperature by measuring the optical intensity from a thermally emissive coating on the sapphire. The potential for greater accuracy than thermocouples led to further development at the National Bureau of Standard (refs. 13,14). A coated sapphire cone was evaluated as an optical temperature sensor for turbine engines (ref. 15). The use of external coatings, however, has limited durability as described by J. Swithenbank (ref. 16). This problem is continuing to receive attention (ref. 1.) by other investigators.

An alternate sensor configuration was proposed by Conax Buffalo in response to a Small Business Innovative Research Solicitation SBIR 86-1 by NASA Lewis Research Center. The innovative probe design is to embed the emissive source inside the sapphire (Ref. 17). The sapphire rod becomes both the lightguide and the sensor shroud. By combining these two functions within the sapphire rod, the probe size is kept small which minimizes response time.

The Phase I Contract (NAS3-25128) demonstrated the feasibility of using the insert technique in a gas flow at temperatures above 1700°C (3092°F). The objectives of the present Phase II Program are to develop a complete sensor system and demonstrate capability to operate in a turbine engine environment.

Specific objectives encompass the development of the full sensor system and address the demanding environmental conditions:

- o Increase probe temperature range, optical emission efficiency and durability
- o Operate the sensor system on gas a turbine during ground test
- o Develop a compact signal processor assembly
- o Support engine demonstration tests with pressure seal, connector and high temperature optical cable and connector
- o Demonstrate system accuracy and reliability by environmental testing

Specific performance goals are listed in Table 1.

TABLE 1. PERFORMANCE GOALS FOR TEMPERATURE SENSOR SYSTEM

PARAMETER	PERFORMANCE GOAL
Measurement Range	600 to 1900°C (1112 to 3452°F)
Operating Limit	2000°C (3632°F)
Accuracy	±19°C (±34°F), ±1% of full scale
Output Resolution	1 degree Celsius (1.8° Fahrenheit)
Time Constant	less than 0.2 s at mass flux of 1000 kg m^{-2} s^{-1} (205 lb $ft^{-2}s^{-1}$)
Environmental Testing	System accuracy verified during temperature and vibration tests Probe assembly tested under temperature, vibration and pressure

3.0 SYSTEM DESIGN

Defining typical operating and environmental conditions for an aircraft turbine engine was the first step in the design process. For a given location in the engine, the measurement process is a sequence of steps, each of which has an impact on the accuracy of the measurement. Tradeoffs are made to select the preferred approach for each step, as well as the overall system performance. Each component is then given a performance budget which allocates the allowable error to achieve the overall system performance goal.

3.1 Gas Turbine Operating and Environmental Conditions

The baseline for the probe design is a military turbine engine as exemplified by the Pratt & Whitney F100 (ref. 18) and GE Aircraft Engines F404 (ref. 19). These engines are a low-bypass, 2 spool turbofan with afterburner. Future requirements were considered with the Integrated High Performance Turbine Engine Technology (IHPTET) Program as a guide (refs. 4, 20).

The turbine inlet region is the most difficult area for probe design due to the combination of the high temperature, pressure and vibration. Typical values for temperature and pressure are listed in Table 2. The velocity of the gas in the combustor is limited to about Mach 0.1 to reduce pressure loss, however, the contraction at the exit of the combustor can raise the velocity to Mach 0.2. The fixed vanes of the first turbine stage form nozzles which increase the velocity to Mach 0.8.

TABLE 2 TURBINE INLET CONDITIONS

DESCRIPTION	MAXIMUM	
	TEMPERATURE ^{o}C (^{o}F)	PRESSURE MPa (psia)
JT9D Burner (ref. 18)	1319 (2406)	2.2 (316)
F100 Burner (ref. 18)	1408 (2566)	2.5 (366)
Present generation (ref. 10)	1316 (2400)	3.4 (500)
Next Generation (ref. 10)	1816 (3300)	3.4 (500)
Experimental Combustors (ref. 20)	1927 (3500)	——

The temperatures on the turbine case and in the aircraft engine compartment are also important design parameters and are listed in Table 3. The F404 and F100 engines have bypass air cooling which limits the case temperature. Other engines or experimental engine cores (high pressure compressor, combustor and high pressure turbine) can have higher ambient temperatures. The engine environment exceeds the temperature rating on conventional fiber optic connectors and cables. Specialized cable and connectors will be required for the optical cable harness used on the hot section of turbine engines.

TABLE 3. EXTERIOR TURBINE TEMPERATURES

LOCATION	MAXIMUM TEMPERATURE ^{o}C (^{o}F)
F15 Aircraft (ref. 7)	
F100 Engine Case	260 (500)
F100 Engine Bay	141 (285)
F18 Aircraft (ref. 6)	
F404 Engine Case	260 (500)
F404 Engine Bay	149 (300)
T56-A-427 Engine (ref. 1)	
Engine Skin	704 (1300)
25mm (1 in) standoff	177 (350)

The turbine engine also creates a high vibration environment (refs. 6,7). At frequencies below 100 Hz the vibration is typically characterized by a displacement with $\pm$0.6 mm ($\pm$0.025 in) a representative value. At higher frequencies the displacement decreases with increasing frequency. The strongest vibrations correspond to hardware frequencies (ref. 20 cites 296 Hz as an example for high pressure turbine) but the envelope of the vibration can usually be approximated by a fixed acceleration of 20 g's from 100 to 2000 Hz. Very high frequencies are associated with the blade passing frequency but these do not usually interact with probe hardware.

There are numerous other environmental factors such as shock, chemical compatibility, salt, fog, etc. Component performance for these factors are usually defined by military specifications. Those specifications which could be applied to temperature sensor hardware are summarized in Appendix A.

3.2 Temperature Relation Between Gas and Probe

The relation between the temperature of the sensing element and the ambient gas is not simple. The probe tip is heated by energy transfer from the gas. If this were the only heat transfer process then the temperature of the probe tip would be equal to the temperature of the gas. The gas temperature would be known from an accurate measurement of the probe temperature.

There are, however, strong temperature gradients in a turbine engine and these induce other heat transfer processes. The probe tip will be cooled by conduction down the probe to a cooler base and by radiation to surrounding engine hardware which is colder than the gas stream. Conversely, radiation from hotter zones (such as a luminous flames) can heat the probe. The result is that the relation between the gas temperature and probe temperature is a complex heat transfer process. A detailed discussion of the theory is outside the scope of this report and can be found elsewhere (refs. 15, 21-23). Specific considerations, as they relate to probe design, are discussed in Section 4.

The response time of the probe to a change in gas temperature is a critical parameter for engine control. At turbine engine conditions thermocouple probes typically have a response time constant of 0.7 to 1.8s (ref. 10) but can be as long as 5s (ref. 7). A faster response of 0.25 would be desirable for stall evasion/recovery (ref. 15). The response time varies significantly with flow conditions as described in Section 4.2.

3.3 Design Approach

The current thermocouple sensor technology used to measure turbine gas temperature represents the state of the art for temperature measurement under severe environmental conditions. Absolute accuracy is less critical than the ability to produce interchangeable sensor systems that reproduce a temperature reading within the tolerance needed for engine control.

Optical systems have the potential to increase the upper temperature limit from 1100 to 1900°C (2012 to 3452°F). The optical approach has further advantages of EMI immunity and the potential of lower weight. To become a viable option for on-engine temperature measurement, the optical system must achieve capability comparable to the thermocouple technology in terms of accuracy, reproducibility, response time, durability, and maintainability.

The first step in the design definition is to select the sensing technique. Alternative measurement techniques have been reviewed previously (ref. 15). This study selected the sapphire lightguide approach and more recent developments do not warrant changing the conclusion. Thermal radiation from a insert in a sapphire lightguide has already been demonstrated for combustion flows up to 1700°C (3092°F). The combination of high temperature, gas velocity and vibration limits alternative probe geometries and, therefore, the radiant insert technique was selected.

The sensor system encompasses all the components necessary to determine the gas temperature and transfer a digital value of that temperature to the engine control. There are many steps in this process, as illustrated in Figure 1, and perturbations to the indicated temperature can be introduced at each step. The design of the sensor system must select the best technique to achieve overall system performance.

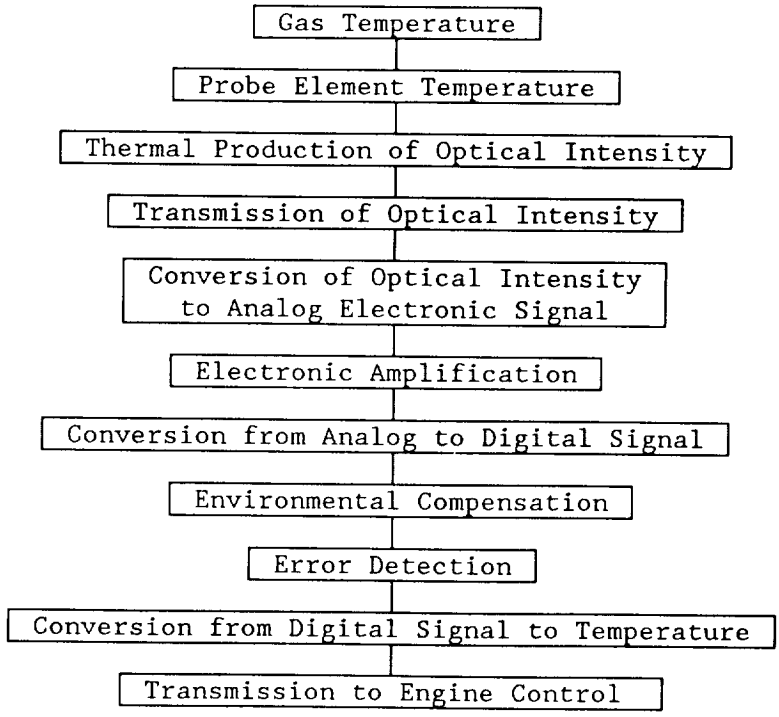

Figure 1. Temperature measurement sequence.

The goal of this program was to demonstrate the feasibility of an optical temperature system for on-engine measurement. The essential components are identified in Figure 2. Listed below each component are the range of environmental parameters selected to demonstrate capability to operate in an engine environment. The interface between the sensor system and engine control would be an optical data transmission path and 28 VDC power connection. To operate the sensor system in stand-alone condition, a display unit was also constructed. The display unit provides a visual indication of temperature and an analog output for recording. It also provides the necessary conversion from AC to DC electrical power.

Two sets of hardware were delivered as part of the contract. To provide additional test opportunities, the probes and cables were designed to work in the Two-Stage Catalytic Oxidation Combustion test facility at NASA Lewis Research Center. The deliverable probes and cables were different in design from the engine test hardware. The probe housing was designed to install in an instrumentation flange. The cable had to be longer to reach the control room, but would be exposed only to moderate temperature in the test cell.

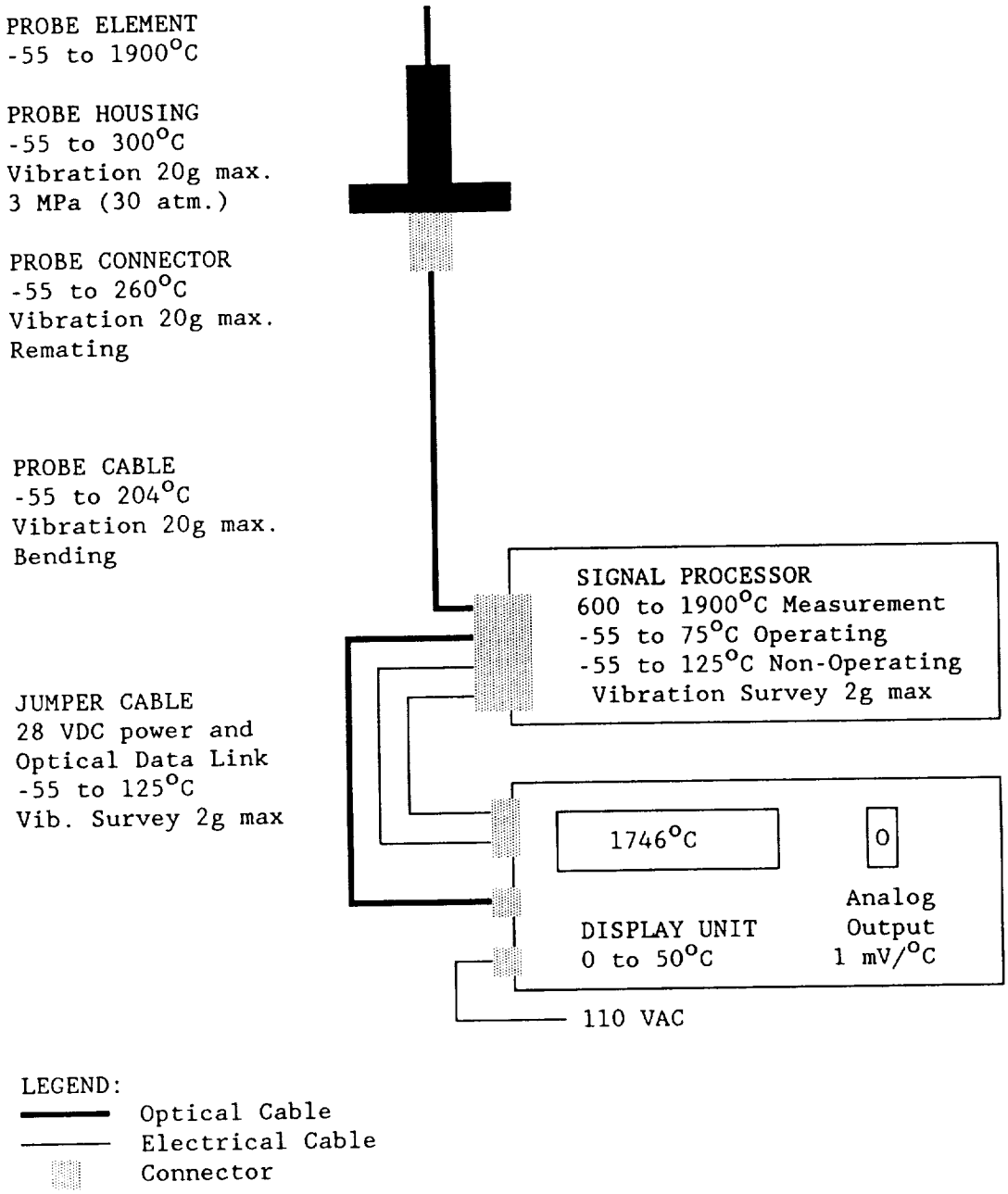

Figure 2. Hardware set to demonstrate suitability for aircraft engine operation.

3.4 Performance Budget

The types of errors that could influence the measurement were grouped into two categories: repeatability and calibration to reference temperature. The environmental factors listed in Figure 2 can perturb the optical signal and, therefore, the repeatability of the indicated temperature value. Reference temperature uncertainty reflects how closely the temperature used in the calibration can be related to true temperature.

The system accuracy is the combination of repeatability and calibration. The program goal is an accuracy of $\pm 1\%$ of full scale or $\pm 19^{o}C$ ($\pm 34^{o}F$). To assess the performance of individual components the system accuracy was divided into a performance budget. Each component, environmental effect, or procedure, which could significantly affect accuracy, was assigned a portion of the total system accuracy. Numerous experiments were then conducted to characterize performance in each category. The budget, experimental data and analysis are described in Section 9.

4. PROBE DEVELOPMENT

The temperature capability of the sensing element was a prime consideration. Probe assemblies were designed for the turbine discharge region of an aircraft engine and a laboratory combustor rig. Analysis included determining the temperature difference between the gas and probe, the resonant vibrational frequency of the sapphire rod, and the sensing element response time.

4.1 Optical Sensing Element

The basic concept of using an insert in a sapphire lightguide had been demonstrated in Phase I. As part of this program, materials were studied to improve the insert with regard to temperature range, emission efficiency and durability.

The selection of the insert material cannot be made simply by studying the melting points of various candidates, as the material may react with combustion gases or sapphire. In addition, the contact between the insert material and the sapphire can reduce the melting point of the sapphire. Thus, it was necessary to experimentally evaluate candidate materials. A study was conducted by Prof. Paul Johnson and his students at Alfred University where furnaces capable of 1900°C (3452°F) were available. Both zirconia and carbon furnaces were used to simulate the oxidizing and reducing conditions in a combustion system. The results of the study are listed in Table 4.

TABLE 4 MATERIAL STUDY AT 1900°C (3452°F)

MATERIAL	MELTING POINT °C (°F)	STABILITY	
		OXIDIZING	REDUCING
Chromium Oxide	2435 (4415)	Good	Good
90% Chromium Oxide 10% Yittria	2435 (4415) 2410 (4370)	Good*	Good*
Cobalt Oxide	1935 (3515)	Reduced	Good
Tungsten Metal	3410 (6170)	Good	Not Tested**
Uranium Oxide	2500 (4532)	Not Tested	Sublimated
Graphite	3652 (6606)	Reaction	Not Tested

*Evidence of liquid stage at high temperature.
**Oxide will form liquid at 1100°C (2012°F).

As expected, several of the candidate materials proved to be unsuitable because of reactivity or melting point depression. Chromium oxide, Cr_2O_3, was selected since experimental studies have shown that mixtures of chromium oxide with aluminum oxide (sapphire is single crystal aluminum oxide) melt at a higher temperature than the sapphire itself (Ref. 24). Prototypes of the sensing element were tested in a burner rig as described in Section 8.2.

Chromium oxide powder was packed into a hole drilled in the end of the sapphire rod. Heating the rod to 1700°C (3092°F) caused the chromium oxide to adhere to the inner surface of the rod. For improved durability it was desirable to seal the hole in the sapphire rod with a piece of 0.5 mm (0.020 in) sapphire rod. A mixture of oxide powders was used to bond the small plug in the hole.

A method to hold the sapphire lightguide was also required at elevated temperatures. To accomplish this, a ceramic collar was fused to the sapphire at the end which will mate with the optical fiber. A complete sensing element consists of a sapphire rod with an insert and plug at one end and a collar at the other.

4.2 Turbine Engine Probe

Mechanical Design. A sensing element and housing were designed for use between the turbine exit and the afterburner. The tip of the sensing element was exposed to the flow for fast response and a ceramic tube was used for support in the hot gas region. The portion of the probe near the flange is exposed only to the cooler bypass air and was made from a nickel alloy. The probe could be separated from the optical cable with a connector at the base of the probe housing.

The probe assembly was designed for a sensing element which slid into the rear of the probe housing as shown in Figure 3. A ceramic collar at the base of the sapphire rod was used to position the sensing element in the housing. A washer, placed between the collar and the metal body of the housing, provided a partial seal and allowed for small variation in the dimensions of the components. Metal felt was selected for the washer material to provide higher temperature capability than could be obtained with plastics.

The sensing element was itself supported by an alumina tube. This tube extended into the hot gas portion of the engine flow and was retained by a larger diameter section held between the metal body and shell. A magnesia ceramic filler was placed between the alumina tube and the metal shell to restrict the vibration of the alumina tube.

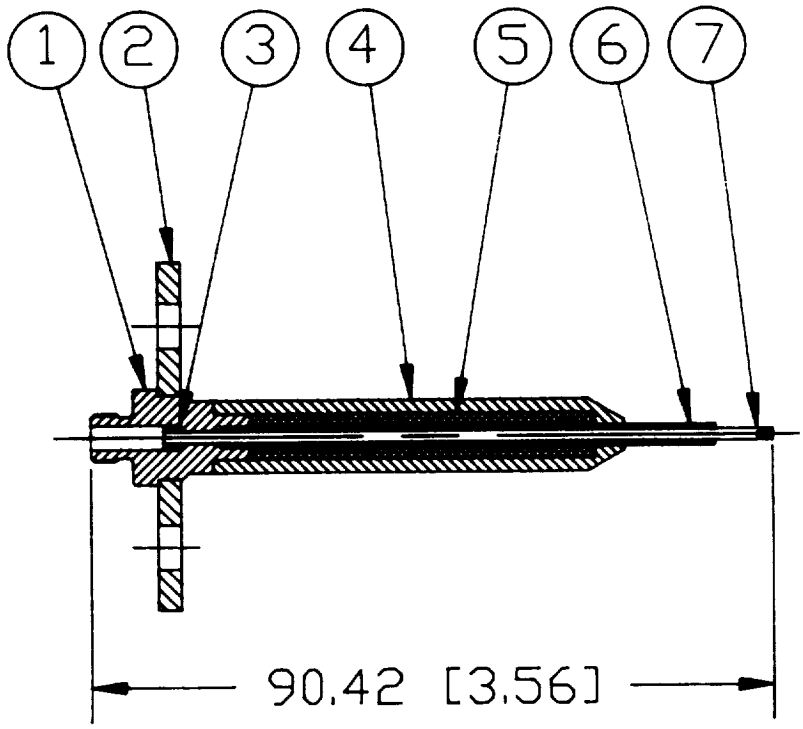

LEGEND
1. Metal Body
2 Metal Mounting Flange
3. Washer
4. Metal Shell
5. Ceramic Filler
6. Alumina Support Tube
7. Optical Sensing Element

Figure 3. Probe design for turbine engine. Units of dimensions are mm(in.).

The connector on the optical cable mated with the threaded portion of the probe housing. The tip of the optical connector came in contact with the sensing element and held the sensing element in place.

Vibration. The durability of the ceramic parts in a high vibration environment is a concern. If the engine vibration induces a resonant vibration in a component, then the probe assembly will be placed under a much higher stress. A vibration study of the sapphire rod was conducted to identify the fundamental resonant frequency.

The resonant frequency of a component changes with the its size, support location, and type of restraint at the supports. The sapphire rod can be treated as a simple beam and the resonant frequency is given by:

$$F = A(I,J)\ [Y\ S/M\ L^4]^{.5} \qquad (1)$$

where:

F	=	Frequency, Hz
A(I,J)	=	Coefficient depending on a support condition (index I) and the vibrational mode (index J)
Y	=	Young's modulus, Pa ($lbf\ in^{-2}$)
S	=	Beam stiffness, m^4 (in^4)
M	=	Mass per unit length, kg/m, (slugs/in)
L	=	Beam length, m (in)

This formula was used to compare predicted values with measurements as listed in Table 5. The agreement was found to be reasonably good using A=0.560 for one end rigidly supported and one end free. The unsupported length is the dominant factor in determining the vibrational frequency.

TABLE 5. VIBRATIONAL FREQUENCY OF SAPPHIRE ROD

Diameter mm (in)	Unsupported Length mm (in)	Calc. Freq. Hz	Observed Freq. Hz
1.27 (0.05)	49.0 (1.93)	698	Approx. 650
1.27 (0.05)	70.7 (2.78)	335	320-350
1.57 (0.06)	57.2 (2.25)	636	602
1.57 (0.06)	70.7 (2.78)	415	370

The probe design required a sapphire rod that was 81 mm (3.18 in) long. The predicted frequency for the 1.27 mm (0.05 in) diameter rod is less than 300 Hz and therefore close to the turbine frequency. It is standard practice to separate the natural frequency of components as far as practical from the primary engine frequencies. For this reason a larger, 1.52 mm (0.06 in) diameter was selected. A further increase to 1.57 mm (0.062 in) would have resulted in inadequate clearance with the housing.

Thermal Analysis. Two aspects of the probe were considered in the thermal analysis: 1. The relation between the gas temperature and the probe temperature, and 2. Probe response time. Both aspects are strongly influenced by the properties of the gas stream and must be analyzed as a heat transfer process (refs. 21-23).

Relation Between Probe and Gas Temperatures. The difference between the gas and probe temperature was analyzed using the method developed by Mossey et al. (ref. 15). In this approach the engine conditions are assumed to vary linearly between idle and full throttle, and these parameters are listed in Table 6. For this study the linear relation was extrapolated to a hypothetical engine with a gas temperature of 1900°C (3452°F). The computer program listed in reference 15 was then used to determine the temperature difference for a 1.52 mm (0.06 in) diameter sapphire rod perpendicular to the gas flow.

TABLE 6. REFERENCE ENGINE CONDITIONS (from ref. 15)

Parameter	Units	Engine Throttle Setting	
		Full	Idle
Gas Temperature	°C (°F)	1700 (3092)	520 (968)
Mass Flow	kg $m^{-2}s^{-1}$ (lb $ft^{-2}s^{-1}$)	825 (169)	122 (25)
Wall Temperature	°C (°F)	871 (1600)	315 (599)
Wall View Factor	Fraction	0.80	0.80
Flame Temperature	°C (°F)	1927 (3500)	1281 (2338)
Flame View Factor	Fraction	0.05	0.02

The temperature difference between the gas and probe is estimated to reach 34°C (62°F) at a gas temperature of 1900°C (3452°F) as shown in Figure 4. The mass flux at this temperature is 942 kg m^{-2} s^{-1} (193 lb ft^{-2} s^{-1}). If the mass flow is reduced, then the temperature difference will increase.

The effective emissivity of the probe tip will vary with temperature but for this study a fixed level of 0.3 was used. Even if the insert is highly emitting this value should give an upper limit to the gas/probe temperature difference. The reason is that the surface area of the insert (viewed from the side) is only 0.17 of the area for the sapphire rod and, therefore, the effective emissivity of the probe tip will be small.

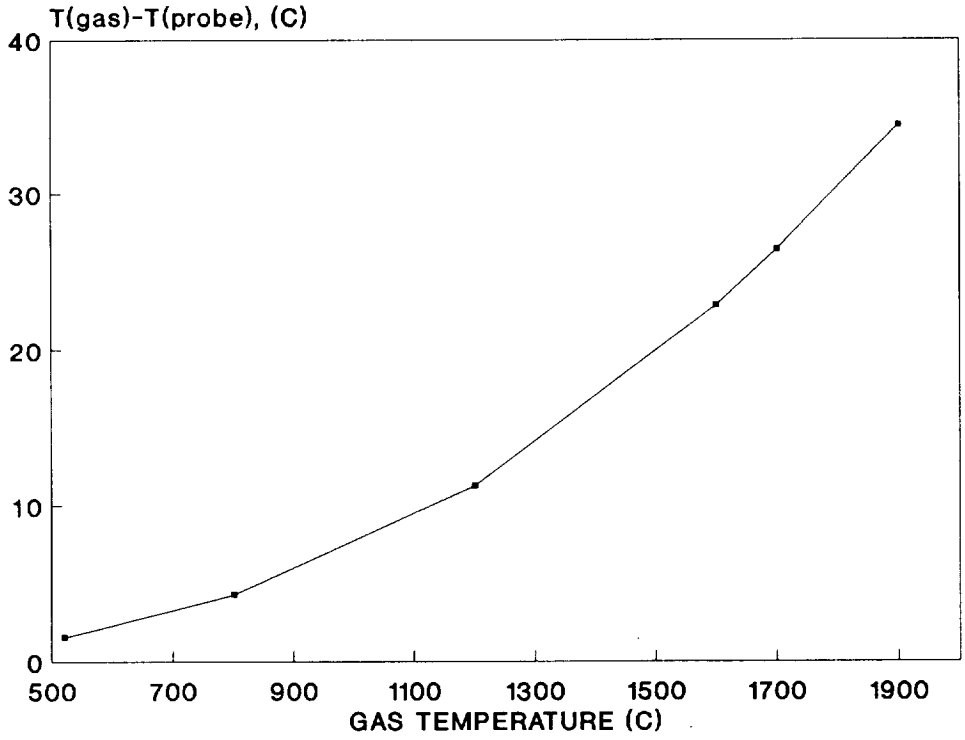

Figure 4. Temperature difference between gas and probe.

Response Time. The response time of the probe was estimated using only convective heat transfer. Effects of radiation will be discussed in Section 9. To derive an equation for response time, it was necessary to simplify the geometry to an infinite cylinder in a cross flow. Then the rate of temperature change for a unit length of the cylinder is equal to the rate of heat transfer to same unit section of the cylinder.

$$(R^2_p)\ L_p\ D_p\ C_p\ d[T_g - T_p] / dt = 2\ R_p\ L_p\ H_g\ [T_g - T_p] \qquad (2)$$

Where

R_p = Radius of probe, m (ft)
L_p = Unit length of probe, m (ft)
D_p = Density of probe, kg m^{-3} (lb ft^{-3})
C_p = Heat capacity of probe, J kg^{-1} $^oC^{-1}$ (BTU lb^{-1} ^oF)
T_g = Temperature of gas, ^oC (^oF)
T_p = Temperature of probe, ^oC (^oF)
H_g = Convective heat transfer coefficient, W m^{-2} $^oC^{-1}$ (BTU h^{-1} ft^{-2} $^oF^{-1}$)

This equation can be rearranged to express the rate of temperature change as a ratio of the heat transfer from the gas to the heat capacity of the probe.

$$\frac{d[T_g - T_p]}{[T_g - T_p]\, dt} = \frac{2\, H_g}{D_p\, R_p\, C_p} \tag{3}$$

Integration of equation (3) yields

$$[T_g - T_p] = [T_g - T_p]_o \, \mathrm{Exp}[-t / \mathrm{Tau}] \tag{4}$$

where Tau, the time constant, is defined as:

$$\mathrm{Tau} = \frac{D_p\, R_p\, C_p}{2\, H_g} \tag{5}$$

The heat transfer coefficient, H_g, is determined in a series of steps starting with the Reynolds number.

$$\mathrm{Rn} = 2U_g\, R_p \,/\, V_g \tag{6}$$

where:

Rn	=	Reynolds number
U_g	=	Velocity of gas, m/s (ft/s)
V_g	=	Kinematic viscosity of gas, M^2/s (ft^2/s)

The Reynolds number is then used in an empirical correlation to determine the Nusselt number.

$$\mathrm{Nu} = A\, [\mathrm{Rn}]^B\, [\mathrm{Pr}]^{1/3} \tag{7}$$

where:

Nu	=	Nusselt number
A,B	=	Empirical constants
Pr	=	Prandl number

The convective heat transfer coefficient is finally determined from the equation:

$$H_g = K_g\, \mathrm{Nu} \,/\, 2R_p \tag{8}$$

where:

K_g	=	Thermal conductivity of the gas, $W\, m^{-1}\, {}^oC^{-1}$ (BTU $h^{-1}\, ft^{-1}\, {}^oF^{-1}$)

Since the composition of the combustion gas can vary, the properties of air (ref. 25) were used to estimate the response time. A time constant of 0.28 s was calculated using the parameters listed in Table 7. This value is higher than the design goal of 0.2 s but design changes to reduce the time constant were not feasible due to the vibration considerations described previously. The actual probe response may be faster than the prediction as described in Section 9.

TABLE 7. ESTIMATE OF RESPONSE TIME

PARAMETER	NOTATION	VALUE USED FOR ESTIMATE
GAS PROPERTIES		
Temperature	T_g	1900°C (3452°F)
Pressure	——	3.04MPa (441psia)
Velocity	U_g	205 m/s (672 ft/s)
Mach Number	——	0.23
Mass Flux	——	1000kg $m^{-2}s^{-1}$ (205 lb $ft^{-2}s^{-1}$)
Kinematic Viscosity	V_g	$1.42x10^{-5}$ m^2/s ($1.53x10^{-4}$ ft^2/s)
Reynolds number	Rn	22,000
Empirical constants	A B	0.193 0.618
Prandl number	Pr	0.7
Nusselt number	Nu	83
Thermal conductivity	K_g	0.134 W m^{-1} $°C^{-1}$ (0.075 BTU $h^{-1}ft$ $°F^{-1}$
Heat transfer coeff.	H_g	7283 W m^{-2} $°C^{-1}$ (1283 BTU h^{-1} ft^{-2} $°F^{-1}$)
PROBE PROPERTIES		
Radius	R_p	1.52 mm (0.06 in)
Density	D_p	3970 kg m^{-3} (248 lb ft^{-3})
Heat Capacity	C_p	1338 J kg^{-1} $°C^{-1}$ (320 BTU lb^{-1} $°F^{-1}$)
RESPONSE TIME		
Time Constant	Tau	0.28 s

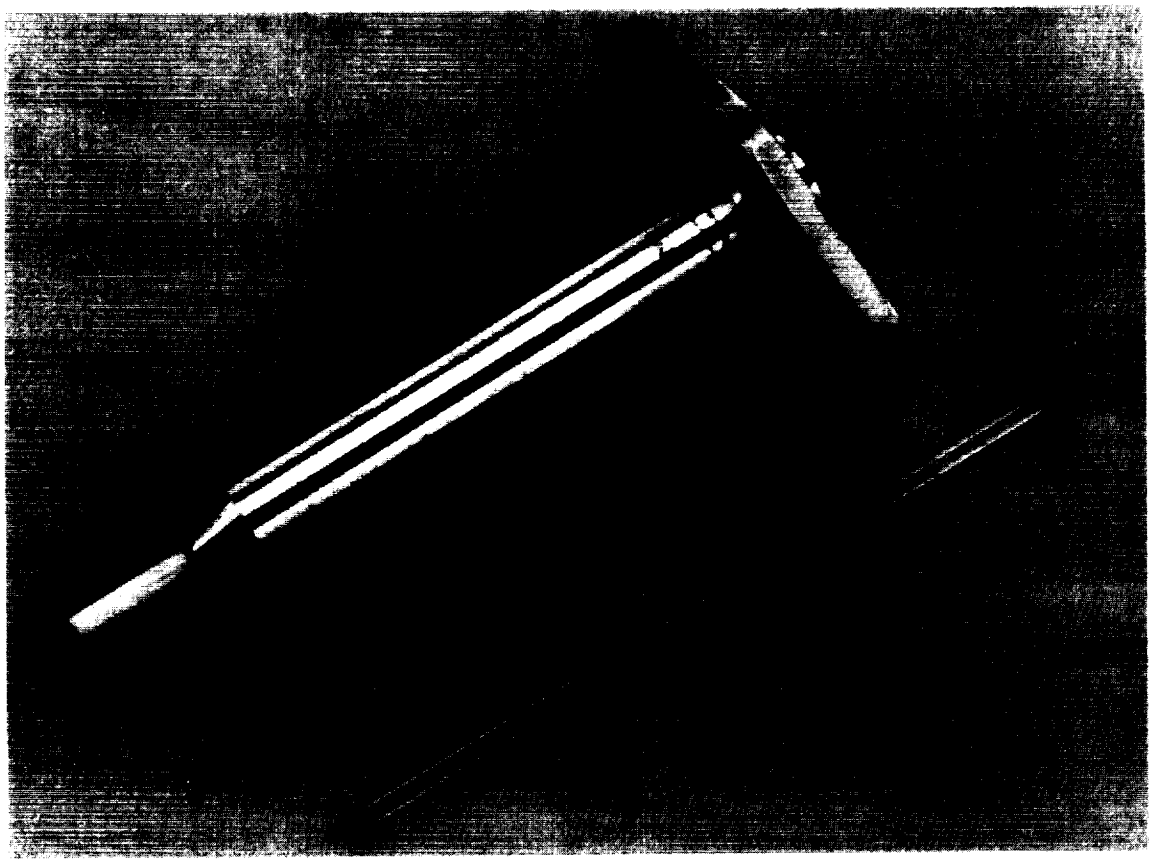

Figure 5. Probe assembly for engine testing.

Fabrication. Two of the engine probes were fabricated for environmental testing on this program. The probe element and housing are shown in Figure 5. The optical quality sapphire was purchased with an optical polish. All subsequent fabrication steps for the insert and collar were conducted at Conax Buffalo. The metal and ceramic parts for the housing were machined. Two welds comprise the assembly of the housing.

4.3 Laboratory Combustor Probe

A laboratory combustion rig will achieve higher temperatures than the exhaust region of turbine engine. To increase the test opportunities, the two deliverable probes were designed for use in the Two Stage Catalytic Oxidation Combustion Test Rig at NASA Lewis Research Center. The temperature requirements were for the sensing element to be capable of operation at 1900°C (3452°F) and for the probe housing to operate in a gas flow at 1650°C (approx. 3000°F).

Design. The design of these probes is shown in Figure 6. The design approach is similar to the engine probe, however, the sensing element penetrates further into the gas stream. The length of the sensing element is 132 mm (5.19 in) compared to 81 mm (3.18 in) for the engine probe. The ceramic support is constructed with silicon carbide to increase resistance to temperature shock.

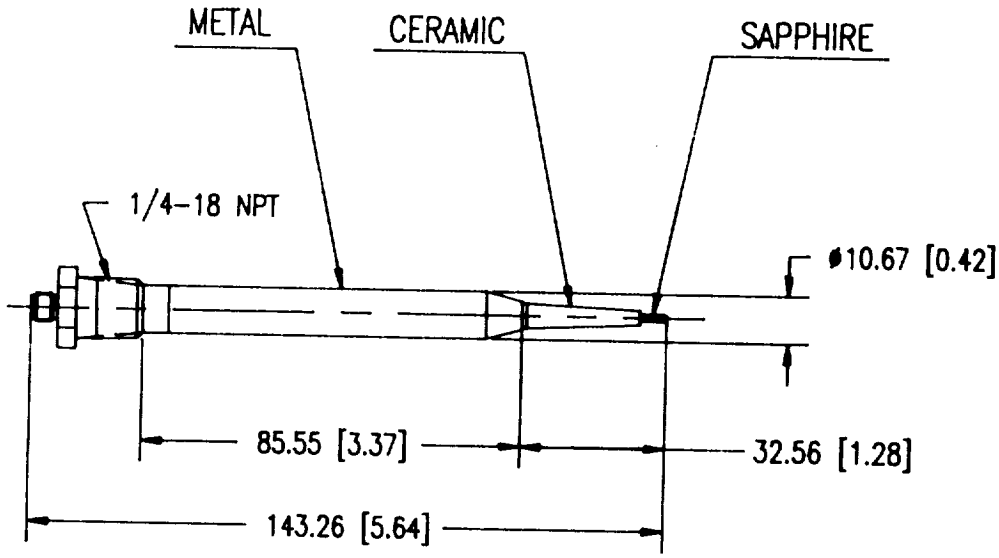

Figure 6. Probe design for laboratory combustor. Units of dimensions are mm (in).

The probes will be installed in a water-cooled instrumentation flange along with other test rig instrumentation. A pipe thread (1/4-18 NPT) is incorporated into the probe housing so that the probe can be installed and removed in the same fashion as other components.

Fabrication. The sapphire rod and silicon carbide support tube were purchased from vendors. The machining and welding were accomplished with in-house facilities. The completed assembly is shown in Figure 7.

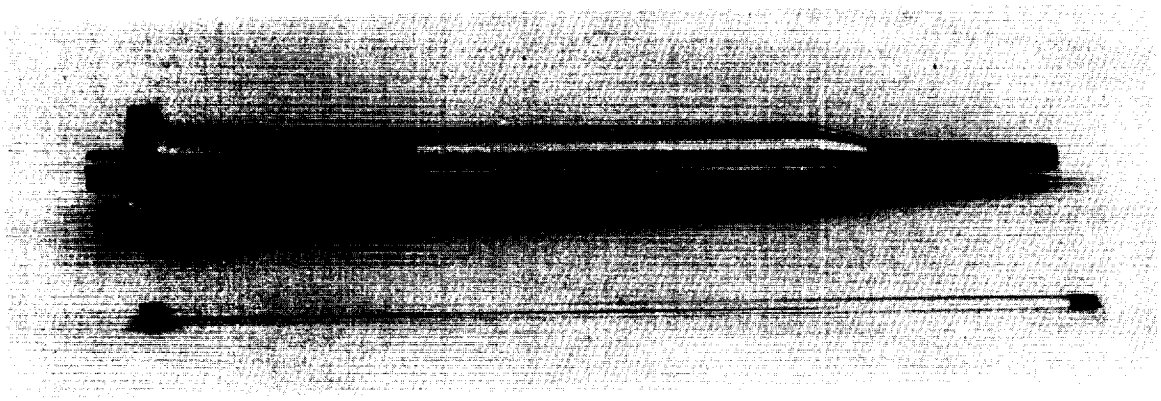

Figure 7. Laboratory Combustor Probe.

5. OPTICAL CABLE DEVELOPMENT

Four types of optical cables assemblies were required for the program. The probe cable for the engine environment must function at temperatures which can reach 260°C (500°F) and vibrational accelerations of 20 g's. The processor assembly requires interior cables which must also meet temperature and vibration requirements. The cable for the combustor probe requires less temperature capability, but must still be rugged enough to be handled like electrical instrumentation cables. Lastly, a cable was designed to provide the optical data link between the signal processor and the display unit.

5.1 Optical Cable for Engine Probe

A design objective for the optical harness was to allow the cable to be demated at both the processor and probe ends. An SMA 906 connector style was selected for the probe end and modified to increase the mechanical strength of the cable jacket attachment. At the processor end, a multi-element circular connector was selected to simulated the interface to an engine control unit. The cable had to be constructed to meet the severe environment encountered by an engine sensor harness. The design of the cable is shown in Figure 8.

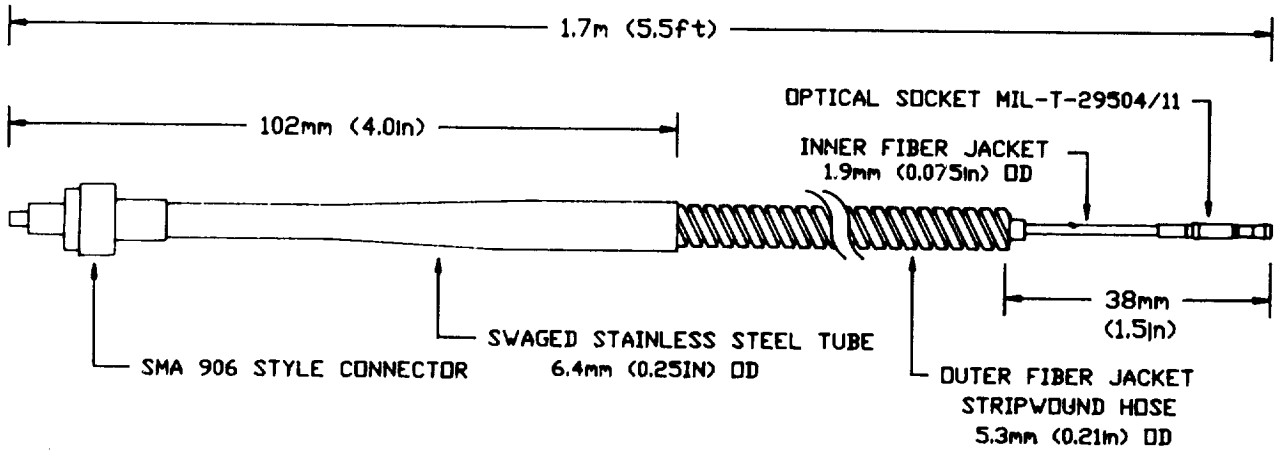

Figure 8. Optical cable for engine testing.

The optical fiber for the cable must have low absorption in the spectral region from 400 nm in the visible through 1900 nm in the infrared. A pure silica core with low OH content was selected. The core fiber size is a compromise between a larger diameter to increase intensity at the processor, and a smaller diameter to allow a small bend radius. A 200 micron, step-index fiber was selected. Lastly, a metal buffer layer was specified over a polyimide buffer to allow brazing to join the fiber to the connector.

The probe connector is modified MIL-C-83522/1 connector which is commonly referred to as an SMA906 fiber optic connector. Both brazing and high temperature epoxy were used as techniques to bond the fiber to the connector. The step down nose of the connector body accepts a plastic sleeve to aid alignment of the connector when it is installed in a bushing. Since the sleeve normally provided would not meet the temperature requirement, it was replaced with a higher temperature material.

For rugged environments, an optical cable is usually constructed with inner and outer jackets. The inner jacket is terminated inside the connectors and provides protection of the fiber from modest loads. The outer jacket joined to the outside of the connector body, is designed to transfer large cable forces to the connector body and not the fiber itself. The outer jacket also provides the primary bend and crush resistance of the cable assembly.

The inner jacket construction was a problem because of the potential for exceeding 260°C (500°F) temperatures at the probe connector. Even aircraft rated optical cables are limited to 200°C (392°F). A custom design was required. A three layer construction of PTFE (polytetrafluoroethylene) tubing, fiberglass sleeving and PTFE tubing were used to protect the optical fiber. The outside diameter was selected to fit inside a size 16 terminus used at the processor end. At the probe end, the inner PTFE tubing was replaced with fiberglass sleeving.

Typical cables are constructed using plastic strength members and jackets. These conventional optical cable materials are not suitable for the environmental temperature range, nor would they control fiber bending adequately. At the probe end, the cable design used a is stainless steel tube crimped to the SMA connector to provide high mechanical strength. This tube could be bent at 90° to reduce the cable height above the flange. The primary protection for the cable was 304 stainless steel stripwound hose. This hose is very flexible down to a bend diameter of 32 mm (1.25 in.) but a large force is required to achieve a smaller diameter. The coils of the hose are interlocked so that it cannot be stretched. These properties of the hose were used to keep pulling or bending load from being transferred to the optical fiber.

The connector selected for the processor end of the cable was a MIL-C-26482 (II) found in commercial aircraft. The connector and termini are similar to (but not interchangeable with) MIL-C-38999 found on military systems. The selection was based on significantly short lead times for the optical termini for the MIC-C-26482 (II). The fiber was bonded to a MIL-T-29504/11 terminus using epoxy and polished with conventional techniques.

Two cables were fabricated for environmental testing. The length was approximately 1.7 m (5.5 ft) and would be representative of the length of an optical engine harness.

5.2 Optical Cable for Combustor Probe

The combustor probe will be installed in a water cooled instrumentation flange. Thus the temperature requirement for the optical cable are less and a working temperature limit of 100°C (212°F) was selected. The cable construction is illustrated in Figure 9.

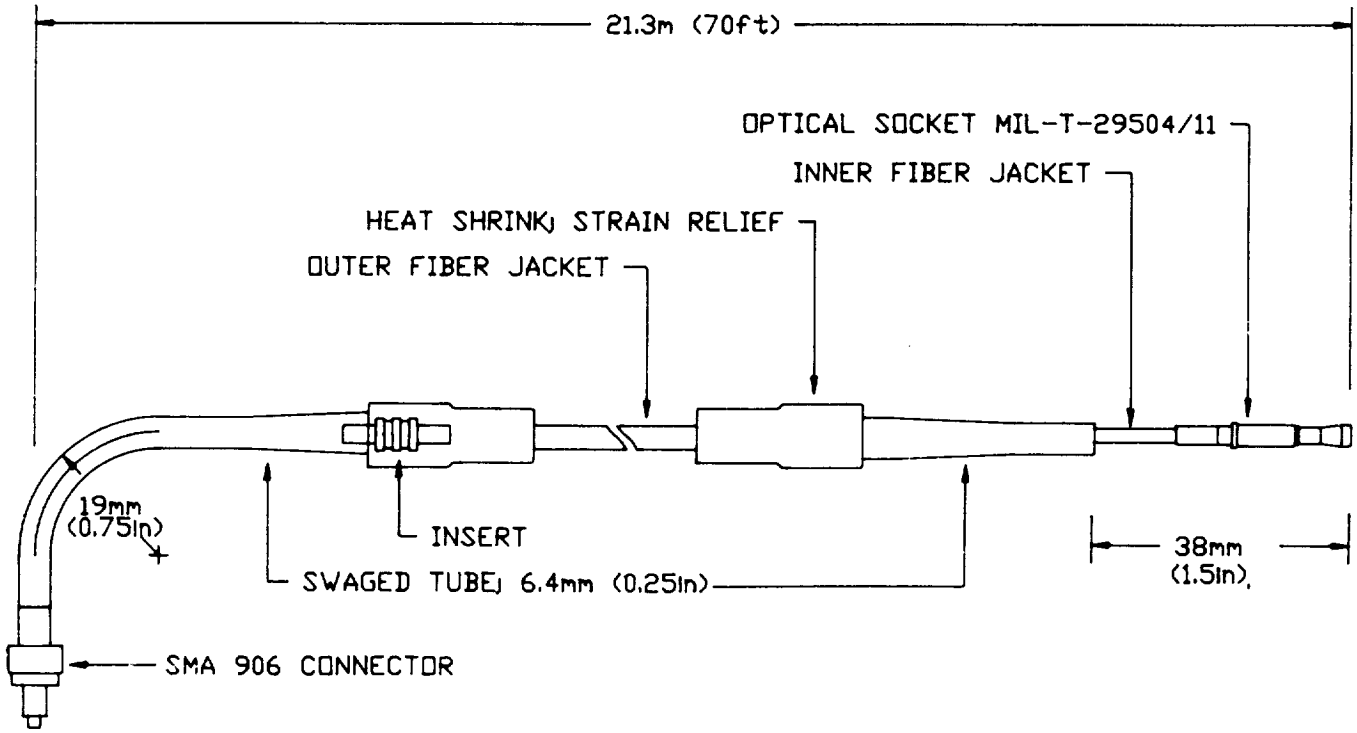

Figure 9. Optical cable for combustor probe.

The step-index optical fiber was commercially available low OH, 200 micron core, step index with 220 micron clad. The fiber had a polymide layer coated with PFA (perfluoroalkoxy copolymer with tetrafluoroethylene) buffer. Near the two connectors, the PFA buffer was stripped off and replaced with an inner jacket with the same construction as the engine cable. The outer jacket was a commercially available item and consisted of three layers: a polyvinal chloride tube, aramid yarn strength members and polyethylene outer jacket. An insert was constructed to joint the outer jacket to the swaged stainless steel tube at the probe end.

The cable was terminated with a stainless steel SMA 906 connector at the probe and an MIL-T-29504/11 terminus at the processor. Both terminations used 200°C (392°F) epoxy and standard techniques. Two cables were fabricated with lengths of 17.7 and 20.7 m (58 and 68 ft.).

5.3 Interior Optical Cables for Signal Processor

A multi-element circular connector was installed in the wall of the signal processor enclosure. This connector simulates the configuration of an turbine engine control unit. Short cables are required inside the processor enclosure to transfer the signals from this connector to the optical components on the circuit board.

The upper temperature requirement was 125°C (257°F) and could be met with commercially available aircraft rated cable. A MIL-T-29504/10 terminus was installed on one end and an SMA 905 connector at the other. Lengths were between .230 to .280 mm (9 to 11 in) and conventional termination procedures used for connectors.

5.4 Optical Cable for Data Link

The display unit was intended for laboratory use only and therefore the cable linking the signal processor to the display uses conventional design. A MIL-T-29504/11 terminus was installed on the processor end and a SMA 905 connector at the display end. The length was approximately 0.6 m (2 ft.) and conventional termination procedure used.

6.0 SIGNAL PROCESSOR DEVELOPMENT

The signal processor converts the optical signal generated by the probe insert in the sensing element to a corresponding digital value indicating the probe temperature. The basic signal processor technology was developed by Conax Buffalo using corporate funds.

The design of the Phase II signal processor is complete. Two signal processor assemblies and two display units have been constructed.

6.1 Conax Buffalo Development

Conax Buffalo, with corporate funds, developed a microprocessor based, signal processor with the following characteristics:

Environmental temperature range of 0 to 50°C (32 to 122°F)
Probe measurement range of 593 to 1371°C (1100 and 2500°F)
Operates from 115 VAC power.

The signal processor consists essentially of 3 printed circuit boards (PCB). Each has a unique function, specifically, analog input signal conversion, microprocessor, and power supply. Also developed was a separate display unit with analog voltage output capability.

A brief description of the key PCB's functions and their unique features is included to provide an understanding of the design required to support the Phase II Program.

The Analog Input Signal Conversion PCB. As stated in previous sections, the optical signal produced by the probe insert is degraded by losses in fiber optic cables and connectors. To minimize the effects of these losses the signal processor computes the temperature based on the ratio of signal intensities in two different spectral bands. This feature is implementated by utilizating a dual (silicon and germanium) photodetector and providing two separate electronic signal amplification channels.

The dynamic range of the optical signal is greater than a single integrated circuit amplifier stage can accommodate so two stages of amplification are provided for each signal channel. The microprocessor will determine which amplification stage signal is appropriate to be used in the ratio to temperature conversion.

Environmental temperature effects on the photodetector and signal amplifiers can cause large electrical signal errors. To account for these signal errors, the temperature of the photodetector is converted to an electrical signal and made available to the microprocessor.

All the signals discussed so far are continuous analog values and must be converted into a digital (binary) form required by the microprocessor. The conversion is accomplished with a 12 bit analog to digital converter. The selection of a 12 bit converter represents a trade off between noise, conversion time, quantizing effects and cost.

Microprocessor PCB. The microprocessor will determine the appropriate signal amplification stage to use for each signal channel (silicon and germanium), and if the minimum signal level for that channel is sufficient to calculate a valid ratio.

To accurately determine probe temperature, the microprocessor must correct each channel signal for the environmental temperature effects on the photodetector and amplifiers. The correction factors are calculated using a second order polynomial and the environmental temperature value acquired from the analog to digital converter. Each corrected channel value is the sum of the correction factor and each channel signal. The coefficients of the polynomial were derived empirically from data collected with the probe at room temperature and shielded from stray light.

Errors caused by environmental temperature effects on each photodetectors spectral range are not significant over this probe temperature range, therefore, no error correction for this phenomena is incorporated in this unit.

The corrected channel values are used to compute the silicon/germanium ratio. If the ratio is within predetermined limits, it will be used with a third order polynomial to calculate the probe temperature. The polynomial coefficients are determined during calibration.

Error checking done by the microprocessor is generally called Built-In-Test (BIT). If the signal channel values are below minimum or if the ratio exceeds the anticipated limits, the microprocessor will output an error code to the display unit.

The microprocessor outputs the temperature value or error code to the display unit via an optical data link. The optical data link allows the signal processor to be remotely located from the display unit.

The microprocessor also provides an external interface to another computer to transfer of calibration data or to monitor the microprocessor internal processing operations.

Power Supply PCB. The Power Supply board contains a linear AC to DC power supply which provides the +5 VDC and $\pm$15 VDC needed by the various electronic components.

Display Unit. The display unit contains two primary PCB's: a display PCB and an analog output PCB.

The display PCB contains a 8 character, 14 segment, light emitting diode display assembly. This display PCB displays the data the signal processor transmits on the optical data link. Normally this is the probe temperature 593 to 1371°C (1100 to 2500 °F) and the units of measure (C or F) or the "less than" symbol if the temperature is outside the probe measuring range. However, if the optical data link should become broken or disconnected the display unit will indicate 'DC'.

The analog output PCB produces an analog voltage proportional to the displayed temperature (3 mV/ °F) that may be used for data acquisition.

Several configurations of this signal processor system were built and tested. The engine testing of the probes described in Section 10 was conducted with Conax Buffalo signal processors.

6.2 Phase II Signal Processor Development

The Phase II goals included the construction of a signal processor that would operate properly at the environmental conditions (for power, vibration and temperature) typically found in existing gas turbine engine control modules.

As stated earlier, the signal processor functional requirements were determined from signal processor development conducted by Conax Buffalo prior to the phase II contract. However, because of this particular application, the following areas were added or improved:

- Inclusion of all signal processing functions on a single PCB.
- Extending the signal processor operating temperature range.
- Extending the measurement temperature range.
- Operating the signal processor from 28 VDC power.
- Extending Built-In-Test functions.
- Ruggedizing the signal processor housing.

Inclusion of all Signal Processing Functions into a Single PCB. Combining the analog input signal conversion, microprocessor and power supply functions onto a single PCB was accomplished. The resulting 5 layer PCB measures 109 x 210 x 1.57 mm (4.31 x 8.26 x .062 in). The digital and analog grounds are separate (except at the analog to digital converter) to minimize ground loop problems. The photodetector and most sensitive analog circuits are located away from digital devices so as to minimized coupling effects.

Extending the Signal Processor Operating Range. In discussions with turbine engine manufacturing personnel it has been determined that typically engine fuel is used to cool the engine control module (and therefor the signal processor) to between -55 and 75 °C (-67 to 167°F). Operating in this environmental temperature range impacted the design in four ways.

1) To operate over this environmental temperature range required the following component changes:

   a) Military grade integrated circuits which have case temperature limits from -55 to 125 ^{o}C (-67 to 257^{o}F) are used.

   b) The photodetector housing was custom made from aluminum as opposed to a commercial product made from plastic.

2) The environmental temperature effects on the photodetector cause a shift in the spectral region to which each detector is sensitive. This shift produced a significant error in each signal channel which became more pronounced as photodetector signals increase (probe insert temperatures increased). To compensate for this error a subroutine was added to multiply the ratio by an additional correction factor. The correction factor is determined using the environmental temperature value and linear equations whose terms are determined during calibration.

3) Empirical data indicated that signal errors for the germanium channel became extremely nonlinear above 50^{o}C (122^{o}F) which eliminated using a polynomial to determine channel correction factors. Therefore, a table lookup subroutine was developed to correct for signal errors in both channels. The values used in the table were determined during the calibration of each unit, and then programmed into the PROM.

4) The PCB is mounted inside of a closed aluminum housing that would prevent adequate convective cooling of the electronic components.

   A 240 node finite element model of the PCB was developed. The worst case thermal input for each component was determined from manufactures specification sheet and distributed over the number of pins on the device. The analysis indicated that the glass epoxy PCB would not have sufficient thermal conduction capability to keep all integrated circuit junction temperatures below their maximum limit.

   From the finite element model it was determined that a 0.51 mm (0.02 in.) thick aluminum heat sink would conduct sufficient heat to keep all integrated circuit junction temperatures within safe limits. Special layout consideration was given to minimizing heat flow near the photodetector and analog circuit components.

   A complete signal processor assembly (PCB inside the enclosure) was placed in an environmental oven to verify the thermal analysis. While the signal processor was operating. The oven was maintained at 85^{o}C (185^{o}F) for three hours. The temperature of the microprocessor, PCB and housing reached 86^{o}C (187^{o}F) confirming the expected small temperature rise.

Extending the Measurement Temperature Range. To achieve a probe operating range of 600 to 1900°C (1112 to 3452°F) a third stage of amplification was added to each signal channel. This added amplifier increased the dynamic range of the optical detector scheme and insures that sufficient signal level is available at 600°C (1112°F) but the system will not saturate at 1900°C (3452°F). The gain of each amplifier stage was adjusted to meet this requirement.

The software routine that determines which amplifier stage to use was modified to include interrogating the third stage amplifier values and to provide a smooth transition in the silicon and germanium channel signals.

Operating the Signal Processor on 28 VDC Power. To meet Phase II requirements for available power the power supply on the signal processor had to be changed. The linear AC to DC power converter was replaced with two DC to DC converters, one to supply the +5 VDC power and a second to supply the +/- 15 VDC power. Since DC to DC converters are switching devices and have the potential to generate excessive conducted electromagnetic interference, suppression filters were added to the input of each DC to DC converter.

Extending the BIT Functions. The BIT function was increased to include an external hardware watchdog timer. If the system is operating properly the microprocessor will issue a pulse to reset the watchdog timer at the beginning of each temperature calculation cycle. However, if the system should get "hung up" and fail to complete the program in 20 ms the watchdog timer will issue a reset pulse to the microprocessor and start the program over again. This loop will continue until the microprocessor completes the program in the allotted 20 ms time.

Ruggedized Signal Processor Housing. The signal processor is housed in a cast aluminum enclosure with dimensions of 220 x 120 x 85 mm (8.66 x 4.72 x 3.35 in). This enclosure was modified to provide a rigid frame on which to mount the PCB. A circular connector conforming to MIL-C-26482 series 2 was mounted on the right hand end of the housing (as seen in the photograph in Figure 10). The MIL-C-26482 connector is a jam nut type that accepts both optical and electrical, size 16, terminals. The contact arrangement is indicated in Table 8. The fiber optic cables appear in Figure 10 as the large diameter cables, whereas the electrical wires have a smaller diameter.

The PCB is securely mounted to the housing on all four sides. Furthermore, there are 6 additional mounting supports distributed across the center region of the board. This mounting technique was selected to minimize the vibration stress and to provide an adequate heat conducting path for the electronically generated heat.

An electromagnetic interference gasket around the cover reduces radiated electromagnetic interference and makes an efficient environmental seal which prevents dirt from contaminating the PCB.

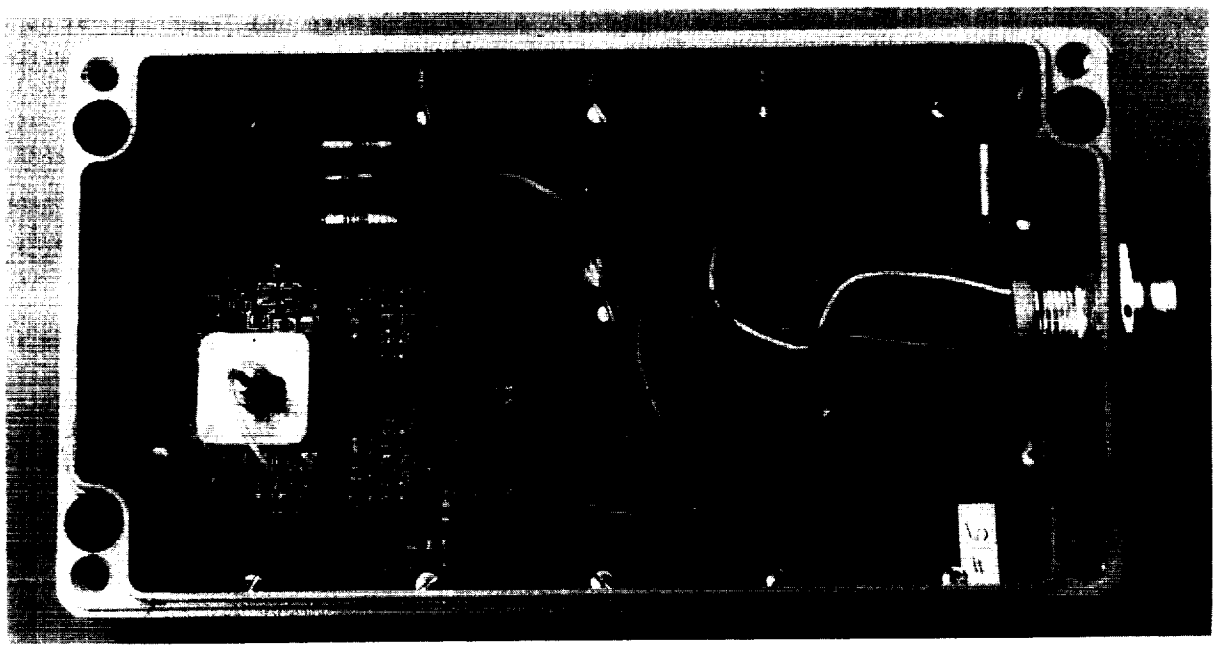

Figure 10. Signal processor circuit board installed in an environmental enclosure.

TABLE 8. CONNECTOR CONTACT ARRANGEMENT

Contact Location	Contact Type	Use
B	electrical	+28 VDC power
C	electrical	-28 VDC power
D	optical	optical data link
E	optical	external computer
F	optical	external computer
G	optical	probe signal
A,I,J,K, and L	none	spare

6.3 Display Unit

The display unit provides the same function as described earlier with the following exceptions; the power supply has been modified to provide the 28 VDC power required by the signal processor, and the analog output has been changed to produce 1 mV/^{o}C output voltage.

6.4 Fabrication

Two complete sensor systems have been manufactured (see photograph in Figure 11) consisting of the following:

2 Signal Processors
2 Display Units
2 Sensor Harness Assemblies
2 Combustor Probes

The sensor harness incorporated into one assembly, the optical cable for the combustor probe, the optical data link cable, and the two 28 VDC power conductors.

To support the early development work a wire wrap version of the signal processor was built. After the PCB design was finished, a board with integrated circuit sockets was assembled and used for software development.

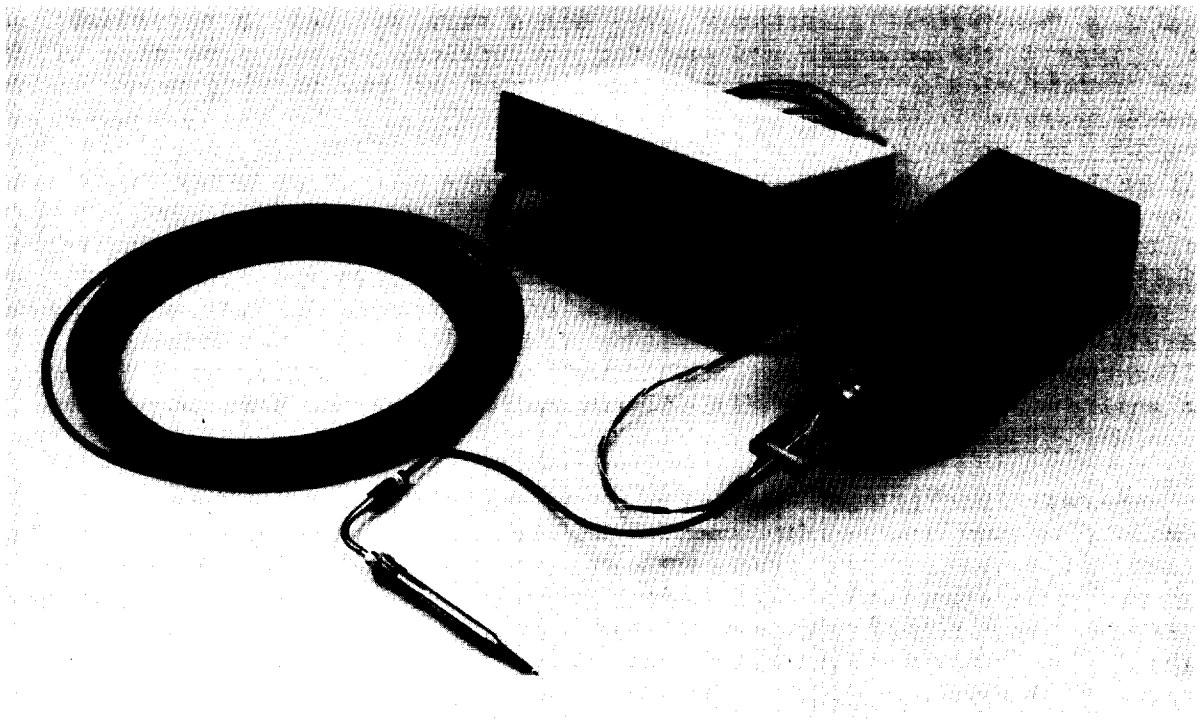

Figure 11. Sensor system for use with laboratory combustor test rig.

7.0 SENSOR SYSTEM CALIBRATION

The calibration procedure determines the necessary constants to relate optical radiation from the probe to its temperature for a specific combination of probe element, optical cable and signal processor. The primary information required is the polynomial data set consisting of paired values of signal ratio and temperature. Additional constants are used in the signal processor for interrelating amplifier gain stages, correcting for environmental temperature of the detectors, and checking signal validity. The calibration procedure is described in this section and the associated uncertainty described in section 9.0.

Polynomial Data Set. The signal processor relates intensity ratio to temperature with a third order polynomial. The polynomial is determined from a least squares fit to experimentally measured pairs of signal ratio and temperature. At 1700°C (3092°F) and above, limitation of the calibration apparatus necessitated that the data pairs be determined theoretically. The use of experimental data wherever possible will result in greater system accuracy.

Calibration Apparatus. A well controlled temperature zone is needed for system calibration. This was accomplished by placing a sintered alumia block in a tube furnace with a 1700°C (3092°F) temperature limit. This block was supported on two thin alumina tubes to minimize heat loss and the resulting temperature gradients. Two holes were drilled in the block, one for a type B thermocouple and one for the optical probe. The mass of the block moderated the thermal transients caused by the varying power to the furnace heaters.

Calibration Procedure. In a turbine engine, the effect of stray light tends to be minimal because most of the background radiation is from hardware which has temperatures much colder than the gas temperature. In the burner region, the flame can have radiation hotter than the downstream gas temperature. For the probe, however, the field of view of the burner is well off axis and therefore little radiation would be transmitted to the detector. The calibration apparatus, on the other hand, presented a different environment. The entire field of view is filled with radiation at the same temperature as the probe.

To separate background radiation from desired insert intensity it was necessary to make two measurements. The first was to measure the stray light by rapidly inserting the probe into the calibration block. At the instant the probe is inserted, the insert is cold and generated no detectable radiation. Any signal measured at this point in time was attributed to stray light. The second measurement was made when the probe has reached the furnace temperature. This signal was the combination of thermal radiation from the sensing element and the stray light. The difference in the two measurements was defined as the intensity from the insert.

The calibration block temperature was limited to approximately 1670°C (3038°F) by the available furnace. Higher temperature could be created in a flame but temperature control was inadequate for calibration purposes. As described in section 9.1, the signal levels were found to follow the expected dependence on blackbody radiation. By normalizing the theoretical ratio of silicon and germanium detector signals to a experimental value, the ratio could be extrapolated to 1900°C (3452°F). Pairs of temperature and theoretical ratio were selected and added to the experimental data set. The polynomial data set was then used to determine the coefficients to a third-order calibration polynomial. These constants are stored in the signal processor.

Amplifier Gain. There were three amplifier stages for both the silicon and germanium detectors. The gain of one stage relative to another must be known so that intensity can be measured continuously over the full dynamic range of the system. These values determined experimentally by recording the outputs from each stage as optical intensity was changed by changing probe temperature. The ratio of the signal from two stages was taken to be the relative gain between these stages and stored in the signal processor.

Dark Current Correction. Even without optical illumination, the silicon and germanium detectors produce an output or dark signal. This dark signal is a reproducible function of detector temperature. It was determined by placing the signal processor in an environmental oven and measuring the dark signal over the range from -55 to 75°C (-67 to 167°F). The necessary correction factor was formulated as a look up table and stored in the signal processor.

Spectral Correction. The spectral response of the detectors also varied with their ambient temperature (see section 9.6). The magnitude of the effect was determined by holding a probe at constant temperature and measuring the optical intensity at 25 and 75°C (77 and 167°F). A scale factor was then determined and loaded into the processor so that an intensity measured at an arbitrary temperature could be converted to an effective intensity at 25°C (77°F).

Validity Checks. The validity of the temperature measurement was checked by using four stored constants derived from an analysis of the calibration data. Lower limits for intensity were selected for each detector below which there was insufficient intensity to adequately determine temperature. The polynomial was valid only over the range of ratios used to determine it. Upper and lower bounds on the ratio were set so that a temperature was calculated only within the calibration range.

8.0 FUNCTIONAL TESTING

Operation of the sensor system on a turbine engine will place temperature and vibration stresses on all of the system components. A series of eleven tests were conducted to characterize the functional aspects of the system components. The effects of environmental conditions on temperature measurement performance are described in Section 9.

8.1 Types of Functional Tests

The environmental effects were different for the probe, optical cable, and signal processor. Test conditions were selected to reflect these different environmental zones and are listed in Table 9. The conditions and procedures were selected to demonstrate that the complete sensor system was suitable for on-engine operation. Full qualification testing would necessarily be more extensive.

8.2 Optical Sensing Element

The sensing element was first tested on a burner rig to assess the combination of temperature, temperature transients, gas velocity, and acoustic effects. The ultimate temperature limit of the sensing element was tested with a laboratory hand torch using a propane/air flame augmented with additional oxygen.

Turbine Burner Test. Arrangements were made to test the sensing elements in a turbine burner flow at Pratt & Whitney, East Hartford, CT. Sapphire rods with inserts were placed in the exhaust of a burner can. A color photograph of this experiment has been published in Reference 26. A detector and amplifier were used to monitor the optical emission from the probe element during the testing. Three sensing elements were tested and the results listed in Table 10.

The time history of the first test is presented in Figure 12. During the first portion of the test, the fuel flow was changed in discrete steps. The corresponding temperature changes resulted in readily identifiable changes in the detector signal levels during the first 750 seconds. After the restart, there was a slight initial drop off which may be the burner stabilizing. The important feature was the steady signal level from 3000 to 7000 seconds. No visual changes to other two rods were observed as a result of the burner tests.

TABLE 9 FUNCTIONAL TESTING

COMPONENT/ PARAMETER	NOMINAL RANGE	ACTUAL RANGE	RESULTS FOR ACTUAL RANGE
PROBE ASSEMBLY			
Temperature of Probe Element	-55 to 1900°C (-67 TO 3452°F)	-55 to 1930°C (-67 to 3507°F)	Pass
Temperature of Assembly	-55 to 300° (-67 to 572°F)	-55 TO 288°C (-67 to 550°F)	Pass
Vibration Survey 10 to 95 Hz 95 to 2000 Hz	±0.64 mm (±0.025 in) 20 g's	Same Same	Pass Pass
Vibration Dwell 310 to 360 Hz	2 hr at 20 g's	Same	Pass
Pressure	3.1 MPa (450 psia)	Same	Pass
OPTICAL CABLE			
Temperature of Cable Assembly	-55 to 150°C (-67 to 302°F)	-48 to 182°C (-54 to 360°F)	Pass
Temperature of Probe connector	-55 to 260°C (-67 to 500°F)	-48 to 300°C (-54 to 602°F)	Pass
Vibration Dwell 30 Hz	±.64 mm (±.025 in) 2 hr parallel 2 hr perpendicular	Same	Pass
SIGNAL PROCESSOR			
Temperature Operating	-55 to 75°C (-67 to 167°F)	Same	Pass
Temperature Non-operating	-55 to 125°C (-67 to 257°F)	-55 to 100°C (-67 to 212°F)	Pass
Vibration Survey Three axes 10 to 74 Hz 95 to 2000 Hz	±.064 mm (±.0025 in) 2 g's	Same Same	Pass* Pass*

* Momentary disruptions of the optical data link between signal processor and display unit were observed at some conditions but not others.

TABLE 10 SENSING ELEMENTS TEST IN BURNER RIG.

SENSING ELEMENT OR PROBE	TEST DESCRIPTION
24758F	Fuel flow changed in 10% steps during first 750 seconds. Flame went out at 750 seconds and was restarted. Steady state at maximum fuel for 6250 seconds. Plug was not in place at the end of test but optical signals were steady.
24758B	The test was conducted at a fixed fuel and air flow rates. After 1000 seconds, the probe was translated in and out of the flame every 60 seconds. The test was continued until there were over 25 cycles on the probe.
7	Air flow increased to get higher temperature. Started with steady state and then went to 60 second cycles for in and out.
P & W Aspirating Probe	Temperature measurements were 1480 and 1510°C (2701 and 2743°F). Pilot measurements were made and Mach number calculated to be .37.
7	Cycle testing for 26 cycles
7	Test to measure probe temperature with pyrometer. Measurements were 1560 and 1539°C (2840 and 800°F).
7	Continued cycle testing for additional 25 cycles.

Probe Element Temperature Limit. The flame from a laboratory hand torch was used to study the upper temperature limit of the sensing element. It was necessary to add oxygen to the propane and air flame to increase the temperature. Even then it was necessary to locate the probe element at the tip of the bright inner cone of the flame to achieve the required temperature. The probe tip was not completely uniform in temperature but the arrangement was sufficient to establish the working temperature limit.

The temperature of the tip was monitored with a two-color pyrometer and the signal processor. The temperature of the flame was increased in four steps. The maximum recorded temperature and observations are listed in Table 11.

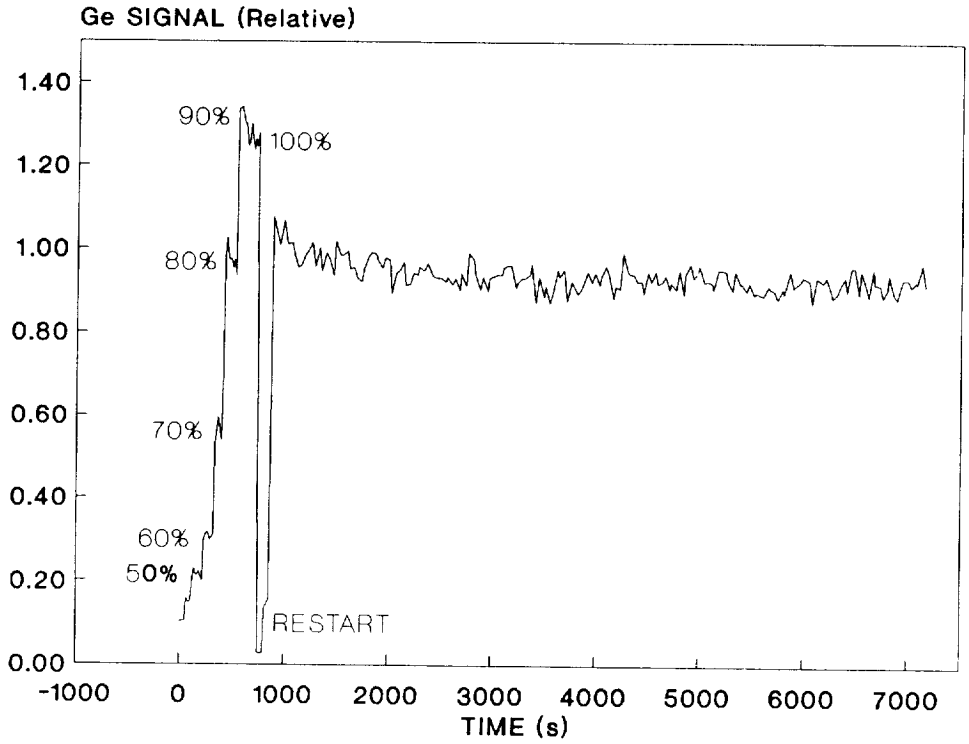

Figure 12. Time history for first burner test. Probe element serial number was 24758F.

TABLE 11 SENSING ELEMENT TEMPERATURE LIMIT

MAXIMUM TEMPERATURE RECORDED		
Pyrometer ^{o}C (^{o}F)	Processor ^{o}C (^{o}F)	REMARKS
1821 (3310)	1867 (3393)	No visual effect.
1873 (3403)	1879 (3414)	Tiny melted zone on rod below insert.
1898 (3448)	1891 (3436)	No visual effect.
1931 (3508)	1922 (3492)	Local melting of seal material on very tip of rod.
1932 (3510)	1927 (3501)	Melting of rod below insert. No visual change to insert.

8.3 Probe Assembly

Temperature. The probe assembly, with the sensing element installed, was located in an environmental oven. A dummy connector was used to hold the element is place. The oven was cooled to -55°C (-67°F) and held for two hours. Visual inspection after the assembly had returned to room temperature showed no damage. In a similar fashion, the probe assembly was heated to 288°C (550°F) with no visible signs of damage.

Vibration. Vibration testing was divided into a survey test and a near resonance dwell. The sinusoidal survey test consisted of ±.64 mm (.025 in) displacement from 10 to 95 Hz and 20 g's acceleration from 95 to 2000 Hz using sweep rate of .25 Octive/min. No visible damage to either the sensing element or housing was observed. The dwell test was conducted at frequencies near the estimated resonance of the sapphire lightguide. Sinusoidal vibration was swept from 310 to 360 Hz at .01 Octive/min and repeated until total time exceeded 2 hours. No resonance was observed and no visible damage to either the probe element or housing was noted.

Pressure. The initial design required only that the optical connector be tightened to a specified torque to achieve a seal. After temperature cycling the assembly some leakage occurred. The probe connector was subsequently modified to provide a spring load on the sealing washer in the probe assembly. The probe assembly was mounted on a test fixture and pressurized with nitrogen. The test assembly was placed under water where any leakage would be observed as gas bubbling from the unit. No bubbles were observed at 2.1 MPa (300 psia) even after temperature cycling the probe assembly and probe connector up to 288°C (550°F). At 3.1 MPa (450 psia) a slight leakage occurred but the rate was less than 6 bubbles per minute and judged acceptable.

8.4 Optical Cable

At least a portion of the optical cable must be mounted on the engine case in the turbine or afterburner section. The temperatures and vibration in this region far exceed the ratings of conventional optical cable components. Tests on the cable and connector at the probe end are described below. The connector at the electro-optics end was tested as part of the signal processor.

Temperature. The optical cable was put in the environmental oven and cycled from -48 to 182°C (-55 to 360°F) for 16 hours. The cable was visually inspected after the test. No problems could be detected visually for either the cable or the probe connector. The connector will reach higher temperature than the cable because it mounts on hardware on the engine case. An additional test of the connector was conducted by heating the connector in a tube furnace from 27 to 316°C (82 to 602°F). Visual inspection showed no evidence of degradation.

Vibration. A probe housing was mounted on the vibration test fixture. The optical cable was installed in the housing and the cable attached 178 mm (7 in.) away from the housing. A short survey scan was conducted to identify the cable resonance near 30 Hz. The setup was vibrated sinusoidally at ±.64 mm (±.025 in.) for two hours on each of two axes (parallel and perpendicular to the axis of the probe housing). Visual inspection did not reveal any damage and there was no detectable change in transmission at 850 nm.

8.5 Signal Processor

Temperature. The circuit board was installed in the housing with RTD's used to monitor the temperature of the housing, microprocessor and heat sink. The output voltage of the DC to DC converter was also monitored. The assembly was put in the environmental oven. The temperature was raised to 85°C (185°F) and normal operating observed after 3 hours. The signal processor was turned off and the temperature increased to 100°C (212°F). Normal operation was observed after the unit had been cooled down to 75°C (167°F).

The assembly was cooled to -55°C (-67°F) and held for 2 hours and normal operation observed with a simulated optical probe input. The unit was also take to -55°C (-67°) without power, held for two hours and then normal operation observed when power was applied.

Vibration. A fixture was fabricated to support the signal processor on all three axes. A sinusoidal vibration survey scan was conducted from 10 to 2000 Hz. The output of the third stage optical amplifier was monitored (both Si and Ge channels) with an oscilloscope. The digital transmission was monitored by watching for the disconnect code on the display unit.

The first test was a sinusoidal sweep at .25 Octive/min with a displacement of ±.064 mm (±.0025 in.) from 10 to 74 Hz and then an acceleration of 2 g's from 74 to 2000 Hz. The processor was vibrated on all three axes with no disruptions of the amplified optical signals observed. Momentary disruptions of the communication links were observed as indicated by "DC" characters on the display unit. These communications disruptions occurred sporadically at frequencies from 36 to 800 Hz in directions along the short axis of the circuit board and perpendicular to the circuit board. None were observed when the vibration was along the long axis of the circuit board.

The second test was conducted with the vibration perpendicular to the plane of the circuit board. The intensity of the vibrational excitation was increased to a displacement of ±.15 mm (±.006 in) from 10 to 88 Hz and an acceleration of 5 g's from 88 to 2000 Hz. No abnormalities were observed for optical or data signals.

9.0 PERFORMANCE TESTING AND ANALYSIS

The reproducibility and calibration of the sensor system is critical to its potential use in engine control. The wide range of environmental parameters can introduce sources of error. Furthermore, calibration at high temperature present numerous difficulties. Extensive tests were conducted to characterize the sensor system and assess system accuracy.

The first level of performance testing was performed to determine the optical characteristics of the system and the probe response time. The second level of performance testing involved the environmental factors which were identified as part of the system design (see Section 3.3). Using this list as a guide, tests were conducted to assess the influence of each parameter on the reproducibility temperature. A performance factor was defined so that data taken under various conditions could be combined to estimate system performance over the full measurement range. The calibration procedure was then analyzed to determine the sources of errors. The combination of reproducibility and calibration represents the overall system accuracy. The assessment of performance was then compared to a design budget (see Section 3.4).

9.1 Optical Characterization

The generation, transmission and detection of the optical signal is a complex process as was illustrated in Figure 1. As a baseline, it was useful to determine the optical signal as a function of temperature. The sensing element was heated in a furnace and measurements made with the optical cable and signal processor. The inherent spectral sensitivities of the silicon and germanium detectors separates the radiation into two spectral regions. The optical signal from the insert was determined by subtracting the detector signal in the dark and the stray light introduced by the furnace. The signal processor selected the appropriate gain stage and the digitized signal is presented in Figure 13.

The measured intensities follow the trend from a theoretical prediction. The theory used black body radiation function weighted with the relative detector response (from the manufacturers specification sheets) as function of wavelength. The summation over wavelength of the weighted terms was taken as the relative intensity at that temperature. This calculation was repeated at 100°C (180°F) intervals. The relative theoretical intensity was normalized to the experimental value measured at 1605°C (2921°F).

The signal levels vary rapidly with temperature and a dynamic range of at least 1,000,000 was required for signal processing. The optical intensity was susceptible to transmission variations, therefore, the ratio of the silicon and germanium signal is used to determine temperature. The ratio is plotted in Figure 14. Since the individual intensities were in good agreement with the theory, the measured and predicted ratios are also in agreement.

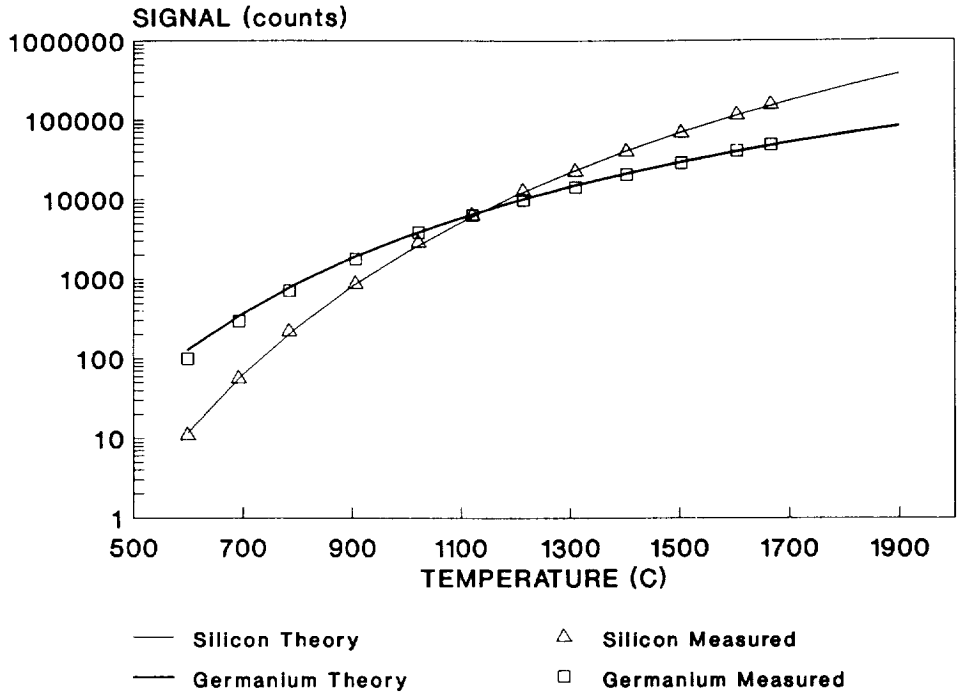

Figure 13. Optical Intensity Measured by Silicon and Germanium Detectors.

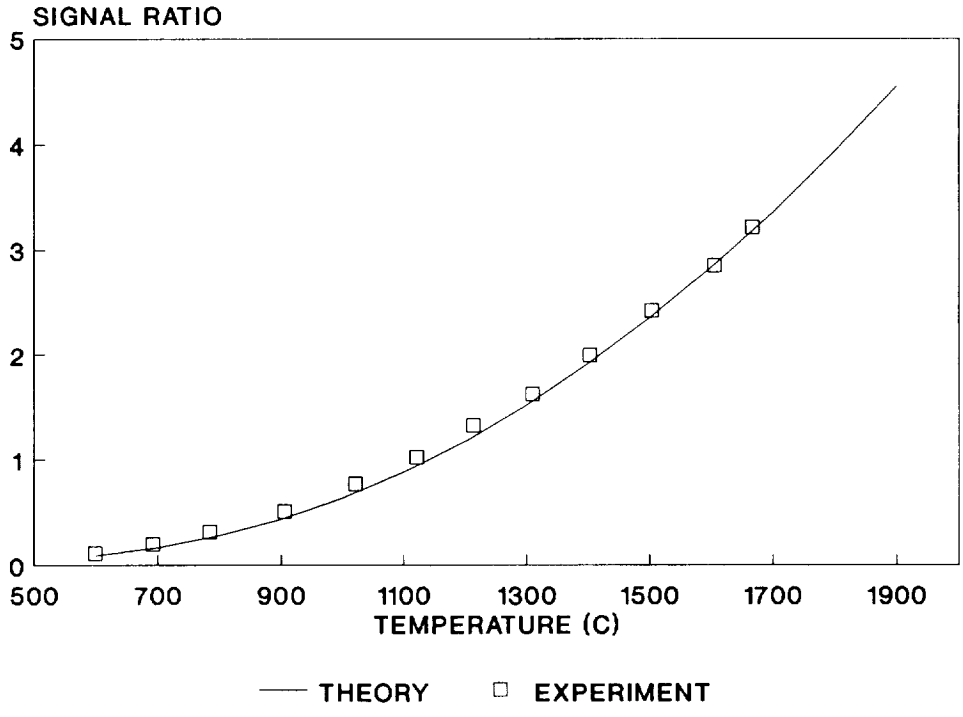

Figure 14. Intensity ratio.

9.2 Response Time

The probe response time defined in Section 4.2 is amount of time required for the indicated temperature to change by $1-e^{-1}$ or 63.2% of a step change in the gas temperature. The response time of the sensing element was the dominant factor since the signal processing time (less than 0.03 s) was small compared to the probe response. The performance goal of 0.2 seconds was specified for a turbine inlet region with a mass flux of 1000 kg m^{-2} s^{-1} (205 lb^{-2} s^{-1}). It was not possible to test at these conditions, so measurements were made at one atmosphere and an analysis used to project the time constant at thirty atmospheres.

The burner test rig described in Section 8 was also used to obtain time response information. The analog intensities on the silicon and germanium detector were recorded as sensing element (#24758A) was rapidly translated into the burner exhaust flow. The nominal conditions were 1.27 mm (0.05 in) diameter rod, 1500°C (2732°F), Mach .37, and 0.10 MPa (14.7 psia).

Detector signals versus time were calculated, assuming the response of the sensing element was described by a single time constant. The theory described in the previous section was used to scale temperature to voltage. Various values of the time constant were tried and the value selected which best fit the experimental data. A time constant of 1.0 s for the silicon detector and 1.1 s for the germanium detector gave a good correlation with the experimental data as illustrated in Figure 15.

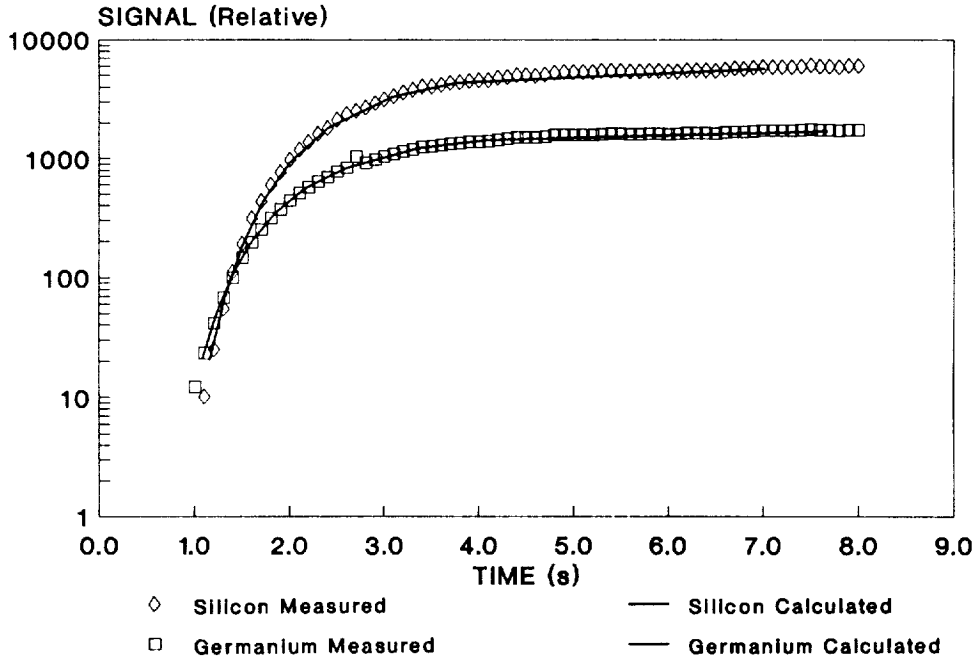

Figure 15. Time response of probe elements.

The value of the time constant was dominated by the heat capacity of the probe and mass flux of the gas. Gas temperature and pressure had only a second order effect. The time constant of the 1.27mm (0.05 in) diameter rod was projected to higher mass flux as illustrated in Figure 16. The same method was then used to project the response time of the larger 1.52mm (0.06 in) diameter rod at a temperature of 1900°C (3452°F).

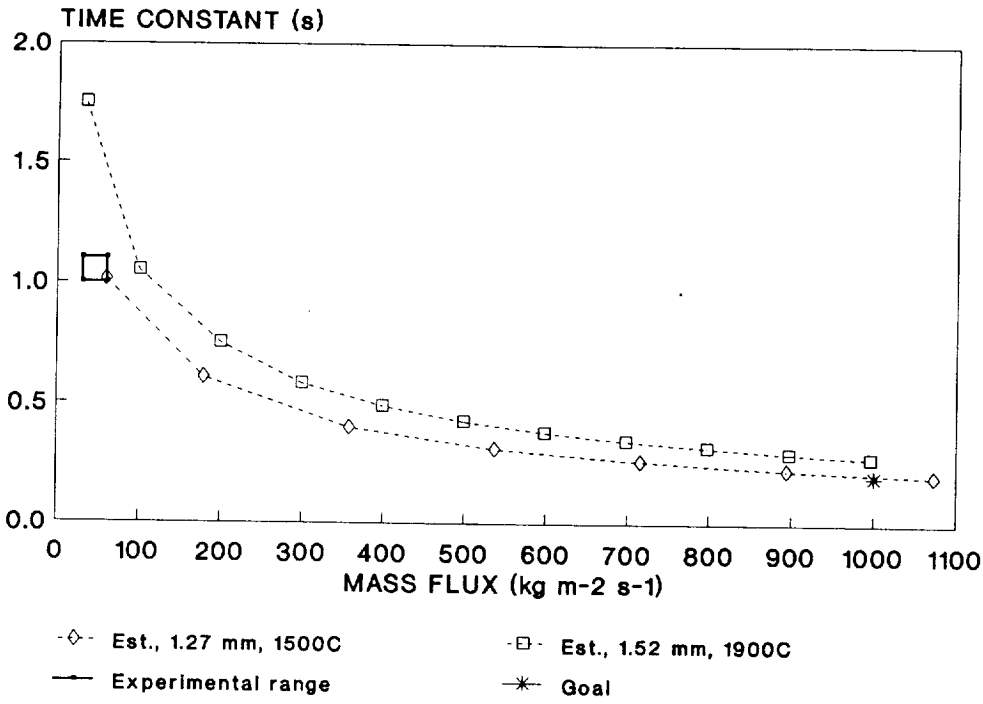

Figure 16. Dependence of time constant on mass flux. Experiment was conducted with 1.27 mm (0.05 in) rod and should be compared to corresponding calculation. Engine probe design uses 1.52 mm (0.06 in) diameter rod and was projected to have a larger time constant.

The goal was a time constant of 0.2 s at a mass flux of 1000 kg m^{-2} s^{-1} (205 lb^{-2} s^{-1}). The time constant predicted from convective heat transfer was 0.28 s. The value could be reduced with a smaller rod diameter, however, for the engine probe this conflicted with vibration requirements. At 1900°C (3452°F) radiative energy exchange would add to the heat transfer (ref.27) and a preliminary assessment indicated that the radiative processes would decrease the response time. It is recommended that the radiative process should be examined in more detail before the rod diameter is changed to decrease response time.

9.3 Performance Factor

Environmental conditions could cause a change in the transmission of the optical components. Absorption or scattering losses can be characterized as a fractional change in the intensity. If this fractional change was the same in two spectral bands then dividing the optical signal in these two bands would produce the same ratio with and without the perturbation. In practice the environmental effects may have a wavelength dependence that will cause the ratio, R, without the perturbation to differ from the ratio R', with the environmental perturbation. A performance factor, f, was defined such that:

$$f = \left| 1 - (R' / R) \right| \qquad (9)$$

Thus, the performance factor represented the fractional change in the signal ratio under the influence of an environmental parameter. It was reasonable to expect that the performance factor would be largely independent of distribution of the intensity within the spectral range of each detector. In this case the performance factor would be independent of the temperature of the sensing element. Under these circumstances the influence of the performance factor could be projected over the full measurement temperature range using the calibration polynomial. The relation between signal ratio and the temperature was fit to a polynomial function, F:

$$T = F[R, C_0, C_1, C_2, C_3] \tag{10}$$

The constants, C_0, C_1, C_2, and C_3, were the polynomial coefficients stored in the signal processor. If an environmental parameter changes the signal ratio to R', then a new value of the temperature would be calculated:

$$T' = F(R', C_0, C_1, C_2, C_3) \tag{11}$$

the associated temperature error would be:

$$T_{err} = T' - T \tag{12}$$

Using equation (9) to relate R and R', the temperature error, T_{err}, was projected over the full measurement range of the sensor system.

Experimentally, the performance factor was calculated from the standard deviation, R_{sd}, in the average signal ratio, $R_{avg.}$:

$$f = Rsd \; / \; R_{avg.} \tag{13}$$

Alternatively, the performance factor was calculated from the a series of measurements

$$f = \left| \; 1 - (R_{md} \; / \; R_{avg}) \right| \tag{14}$$

where R_{md} was the ratio for the condition with the maximum deviation from the average. The absolute value was used to insure that f is positive and the corresponding temperature error was positive. When temperature errors for multiple effects were combined they were presumed to be additive. Thus, the worst case was assumed in which individual errors combine to produce the maximum possible total error.

9.4 Probe Testing

The sensing element should produce the same signal ratio each time it is exposed to the same temperature environment. The short term reproducibility was determined simply by comparing ten measurements where the sensing element was inserted and removed from the cavity of a blackbody light source (see Table 12). The blackbody source was used because of its stability, but this unit still varied by more than $1^{o}C$ ($1.8^{o}F$) during the course of the testing. Thus, the performance factor was made up, in part, of apparatus effects not directly due to the insert in the sensing element.

TABLE 12. PROBE REPRODUCIBILITY

CONDITION	NO. OF SAMPLES	AVERAGE RATIO	STANDARD DEV.	PERFORM-ANCE FACTOR
Short Term	10	0.3398	0.0004	0.0014
Long Term	Est.	——	——	0.0050

Determining the long term reproducibility presents a greater problem in achieving a stable measurement apparatus. Observations made during other testing have not shown a distinguishable change in the emission ratio from the insert. The performance factor of 0.005 has been assumed until more information become available. The performance factors listed in Table 12 were used to project the temperature error over the measurement range of the sensor system (see Figure 17).

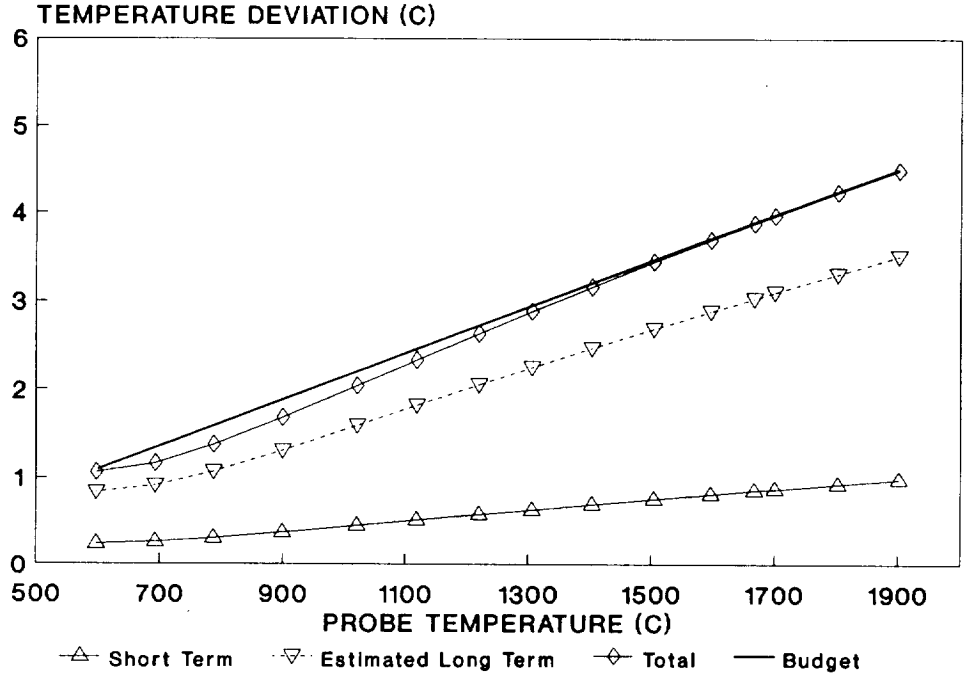

Figure 17. Reproducibility of Probe

9.5 Cable Testing

Perturbing influences on the cable included remating connectors, bending, temperature and vibration. These factors could cause a change in the transmission of the optical intensity. To obtain sufficient resolution of the signal change, the output of the analog amplifier was measured using a multimeter with at least 5 digit resolution. Multiple readings were taken and averaged to further refine the measurement. Vibration was tested in combination with the signal processor and is described in Section 9.6.

Remating. The connector remating test was conducted by measuring the intensity on both the silicon and germanium detectors, disconnecting and reconnecting the connector, and then remeasuring the two intensities. The ratio was calculated for each cycle and the performance factor was calculated from the standard deviation of the ratio. This data is summarized in Table 13. The connector at the probe end was a modified SMA 906 style and at the processors end it was a MIL-T-29504/11 terminus in a MIL-C-26482 (II) connector.

TABLE 13. CONNECTOR REMATING

CABLE END	NO. OF SAMPLES	AVERAGE RATIO	STANDARD DEV.	PERFORM-ANCE FACTOR
Probe	5	0.3716	0.0008	0.0022
Processor	10	0.6321	0.0003	0.0005

Bending. The full numerical aperture of the optical cable was used to transmit the optical intensity from the probe. With short cable lengths the mode distribution within the cable could be affected by bending. Intensity measurements were made with the cable in a relaxed condition, and then formed into a 360° loop. The loop was characterized by its smallest radius but was not exactly circular. As listed in Table 14, the intensity decreased to 87% at a 16 mm (0.62 in.) radius, while the ratio changed only 1%. If the performance factor calculated for a bend radius of 51 mm (2 in) were used then the temperature error would be unacceptable. For purposes of error analysis the bend radius was limited to 102 mm (4.0 in). The performance factor was not measured for this radius but was estimated to be half of the value for the 51 mm (2 in) measurement.

TABLE 14. CABLE BENDING

RADIUS mm(in)	NO. OF SAMPLES	INTENSITY, Volts		RATIO	RELATIVE RATIO	PERFORM-ANCE FACTOR[a]
		Silicon	Germanium			
Straight	10	1.2374	3.4627	.3573	1.0000	——
102(4.0)	Est.	——	——	——	——	0.0046
51(2.0)	10	1.1964	3.3791	.3540	0.9908	——
38(1.5)	10	1.1795	3.3475	.3523	0.9860	——
25(1.0)	10	1.1505	3.2681	.3520	0.9851	——
16(0.6)	10	1.0691	3.0120	.3549	0.9933	——

a. Performance factor estimated using half the value for a 51 mm (2.0 in) cable bend radius.

Temperature. The optical cable will be subjected to high temperature since it is mounted just outside the engine case. Correspondingly it must also function for a cold start condition at -55°C (-67°F). The optical connector at the probe end of the cable has a wider range of temperature than the main portion of the cable and therefore was tested separately. The optical connector at the processor end of the cable was temperature tested as part of the processor.

A probe housing was modified so that the sensing element could be installed in the blackbody without the metal housing entering the blackbody cavity. The probe connector was heated with a small tube furnace. Alternatively, gaseous nitrogen was used to cool the connector and 152 mm (6 in.) of cable. Thermocouples were placed on the connector and cable to monitor local temperatures. When the connector was at -53°C (-63°F), the cable was at -92 and -68°C (-133 and -90°F) at distances of 57 and 114 (2.3 and 4.5 in.) from SMA connector nut. The measurements are summarized in Table 15. Once the engine is operating the probe connector will be heated. The performance factor, 0.0017, was calculated from the maximum deviation of the ratio from the average ratio over the range from 27 to 316°C (81 to 602°F).

TABLE 15. CABLE TEMPERATURE

TEMP. °C(°F)	NO. OF SAMPLES	INTENSITY, VOLTS		RATIO	R_{md}/R_{avg}	PERFORM-ANCE FACTOR[a]
		Silicon	Germanium			
PROBE CONNECTOR HEATED						
27 (81)	10	3.6086	8.2401	.4379	1.0017	0.0017
96(205)	10	3.5850	8.2090	.4367	0.9989	——
204(400)	10	3.5905	8.2184	.4368	0.9993	——
316(602)	10	3.6001	8.2332	.4372	1.0001	——
	AVG.			.4372		
PROBE CONNECTOR COOLED						
12 (53)	10	2.0390	5.4233	.3753	1.0015	N/A
-53(-63)	10	1.5763	4.1650	.3784	1.0081	N/A
-2 (29)	10	2.1432	5.7635	.3718	0.9904	N/A
	AVG.			.3754		
760MM (30 IN.) SECTION OF CABLE						
-56(-69)	15	2.2176	5.9191	0.3746	0.9977	——
25 (77)	30	2.2510	5.9868	0.3759	1.0013	0.0013
208(406)	15	2.2491	5.9847	0.3758	0.9999	——
	AVG.			0.3754		

a. Performance factor calculated with maximum ratio deviation for environmental temperature above 25°C(77°F).

To determine the effects of temperature on the optical cable a 760 mm (30 in) section was placed inside an environmental oven. Intensity was measured at ambient, -56°C (-69°F), and 208°C (406°F), with the environmental oven temperature cycled three times. The data is summarized in Table 15. The performance factor, 0.0013, was calculated from the maximum deviation of the ratio from the average over the range 25 to 208°C (77 to 406°F).

Comparison with Budget. The performance factor for the various cable effects were converted into corresponding temperature deviations. Figure 18 presents the errors associated with individual processes and the total for the cable. The combination of errors exceeded the budget by 1.7°C (3.1°F). The bending of cable has the largest perturbation, and additional measurements are needed to adequately characterize the effects of bending.

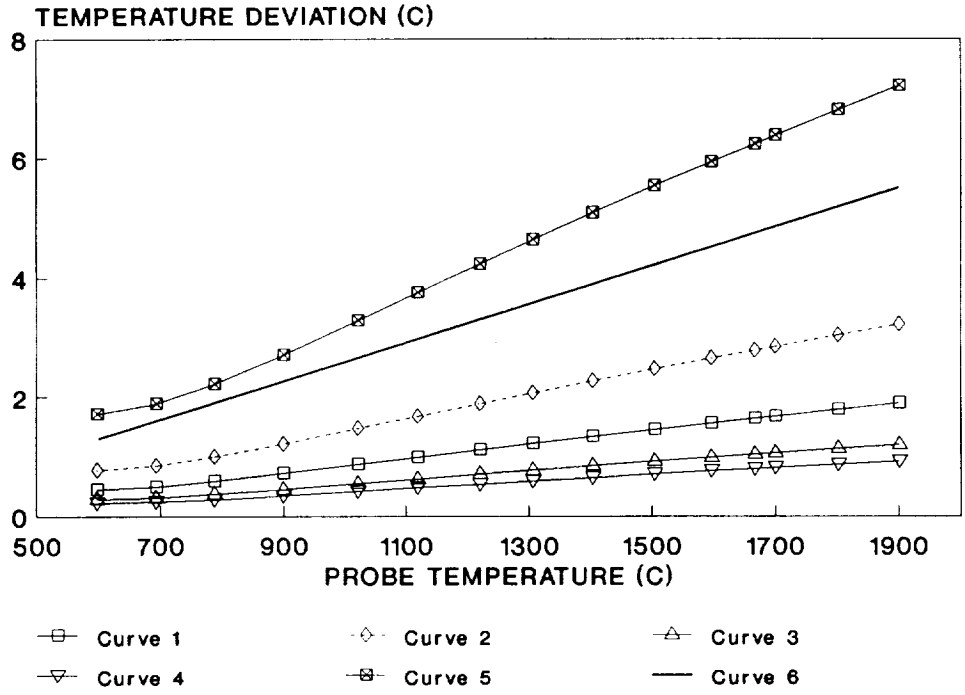

LEGEND

Curve 1. Remating of both optical connectors

Curve 2. Estimated cable bend for 360° loop in cable of 102 mm (4.0 in)

Curve 3. Probe connector over temperature range of 27 to 316°C (81 to 602°F).

Curve 4. Cable over temperature range of 25 to 208°C (77 to 406°F)

Curve 5. Combined environmental effects on optical cable.

Curve 6. Budget.

Figure 18. Reproducibility for optical cable.

9.6 Signal Processor Testing

The signal processor was susceptible to three primary types of perturbations, polynomial curve fit, temperature and vibration. The curve fit reflected the difference between the data set of temperatures and and corresponding signal ratios and the temperature calculated with the polynomial fit to this data. The signal processor was tested with a case temperature from -55 to 75°C (-67 to 167°F) to simulate the temperature of the fuel cooled heat sink. For this program it was assumed that the signal processor would be mounted on vibration isolators which would attenuate the engine vibration by a factor of ten.

Polynomial Curve Fit. Pairs of temperature and ratio were fit to a third order polynomial which could be rapidly evaluated by the signal processor. The temperature calculated with the polynomial differed from the data set from which it was created and this difference was defined as the polynomial error (see Table 16).

TABLE 16. POLYNOMIAL CURVE FIT

POLYNOMICAL DATA SET			CALCULATED TEMPERATURE		POLYNOMICAL DEVIATION	
TEMPERATURE °C	(°F)	RATIO	°C	(°F)	°C	(°F)
598.0	(1108.4)	0.112	597.4	(1107.4)	0.6	(1.0)
692.0	(1277.6)	0.194	692.4	(1278.4)	0.4	(0.8)
784.0	(1443.2)	0.314	787.6	(1449.7)	3.6	(6.5)
905.0	(1661.0)	0.503	899.6	(1651.3)	5.4	(9.7)
1021.0	(1869.8)	0.764	1021.7	(1869.3)	0.3	(0.5)
1120.0	(2048.0)	1.018	1118.6	(2045.6)	1.4	(2.4)
1213.0	(2215.4)	1.323	1220.2	(2228.4)	7.2	(13.0)
1309.0	(2388.2)	1.617	1306.6	(2383.9)	2.4	(4.3)
1403.0	(2557.4)	1.988	1404.2	(2559.5)	1.2	(2.1)
1503.0	(2737.4)	2.415	1504.5	(2740.1)	1.5	(2.7)
1605.0	(2921.0)	2.847	1596.2	(2905.2)	8.8	(15.8)
1666.0	(3030.8)	3.210	1667.2	(3033.0)	1.2	(2.2)
1700.0	(3092.0)	3.388	1700.4	(3092.7)	0.4	(0.7)
1800.0	(3272.0)	3.969	1801.8	(3275.3)	1.8	(3.3)
1900.0	(3452.0)	4.589	1900.8	(3453.4)	0.8	(1.4)

Environmental Temperature. Much of the signal processing is handled in digital format and therefore not directly influenced by temperature. The optical detectors, and amplifiers, and analog to digital converter are all influenced by the temperature of the local environment but the detector properties exhibit the strangest sensitivity.

Environmental Temperature. The detectors produced an output without incident light and the amplified value is labeled dark signal. The dark signal was normalized to the 25°C (77°F) and plotted versus detector temperature in Figure 19. For the silicon detector the dark signal decreased 16% at -55°C (-67°F) and increased 5% at 75°C (167°F). The behavior of the germanium detector is more complex, the dark signal was reduced 9% at the low temperature but was also reduced by 8% at the high temperature. A possible explanation for this phenomena was that, while the germanium detector produced a dark current that increased with temperature, the detector's shunt impedance decreased with temperature, thereby "short circuiting" the output signal. The first stage amplifier tended to compensate for this effect, to some extent, because as the shunt impedance decreased, the gain of the amplifier stage increased. However, above approximately 50°C (122°C) the reduced shunt impedance dominated and thus output signal decreased. The detector temperature was measured and a correction implemented in software to account for the dark signal and its environmental temperature dependence.

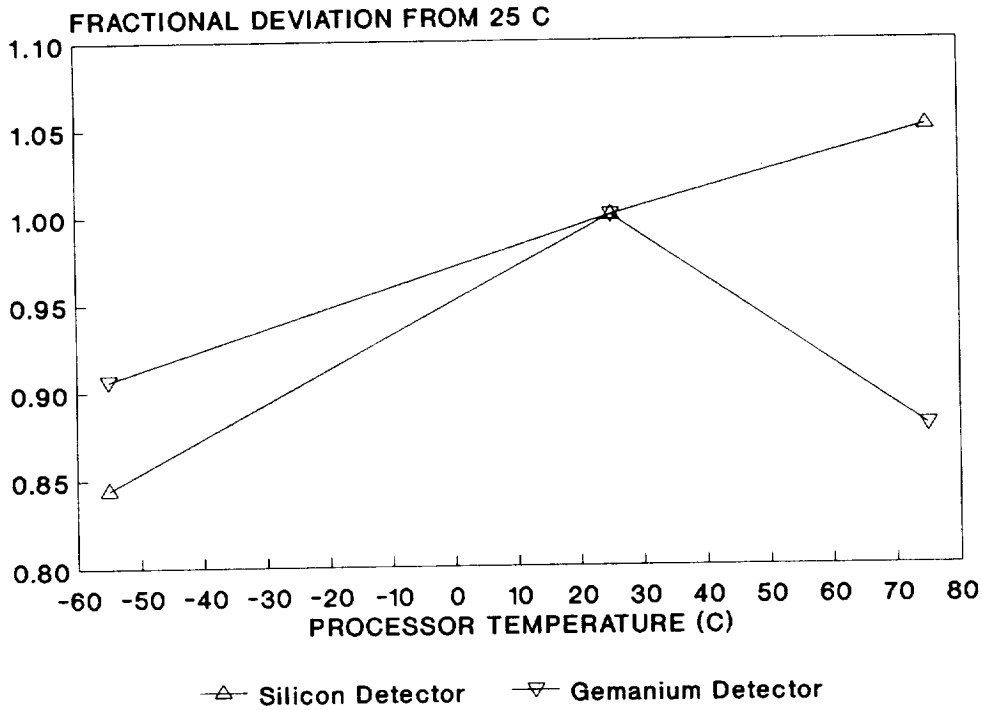

Figure 19. Dark signal variation. Individual curves have been normalized to value at 25°C (77°F).

The spectral response of the detectors also has a sensitivity to environmental temperature. Using a probe temperature of 1200°C (2192°F) the optical signal, corrected for dark signal, was measured at three temperatures. Figure 20 shows the relative change with the signal normalized to 25°C (77°F). The effect is significant with the silicon detector varying from -38% to 36% and the germanium detector from -35% to 28%. Using a ratio of silicon to germanium partially compensates for the variation but leaves a residual -9% to 8% effect. Accordingly, a correction was made for the spectral effects introduced by the environmental temperature of the processor.

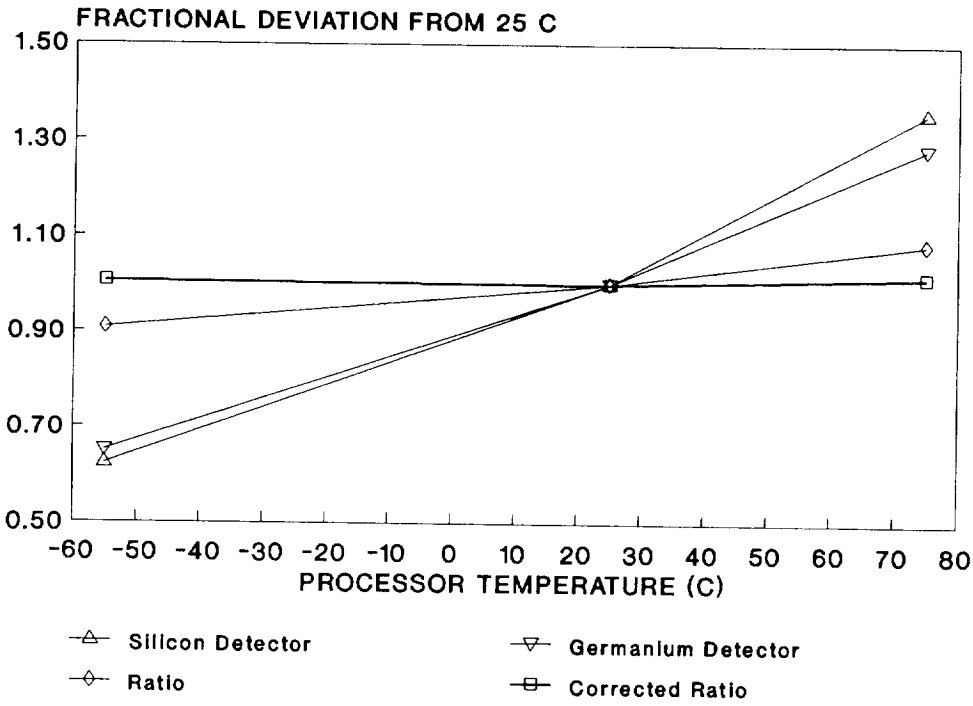

Figure 20. Optical Signal Variation. Individual curves have been normalized to value at 25°C (77°F).

The performance of the environmental temperature correction processor was measured over a 600 to 1650°C (1112 to 3002°F) range of probe temperature and a -55 to +75°C (-67 to 167°F) range of processor temperature. This was accomplished by locating the probe in a high temperature furnace and the processor in an environmental oven. Probe and processor temperatures were varied independently. A sapphire rod with a platinum cap was used as the sensing element to eliminate the need to make corrections for stray light.

Three readings were taken at each combination of probe temperature and processor temperature. At a given environmental temperature the variability of the reading has a standard deviation of only 1.1°C (2.0°F). An average ratio was calculated from the six values in 25 and 75°C (77 and 167°F) data sets. The -55°C (-67°F) data was not included since the processor is seldom operated at this condition. Table 17 summarizes results with the ratio entries being the largest deviation from the average. The performance factor was then calculated from the larger deviation of the 25 and 75°C (77 and 167°F) data sets. Thus, this performance factor should represent the worst case effect of the environmental temperature on the processor.

TABLE 17. PROCESSOR TEMPERATURE EFFECTS

PROBE TEMPERATURE °C (°F)	NO. OF SAMPLES	RATIO[a]	AVG. RATIO 25-75°C (77-167°F)	PERFORM-ANCE FACTOR[b]	REMARKS
PROCESSOR AT 25°C (77°F)					
600 (1112)	3	0.1694	0.1618	——	
700 (1292)	3	0.2088	0.2126	0.0181	
800 (1472)	3	0.3020	0.3094	0.0245	
900 (1652)	3	0.4292	0.4401	0.0255	
1000 (1832)	3	0.5909	0.6029	——	
1100 (2012)	3	0.8022	0.8140	0.0147	
1200 (2192)	3	1.0475	1.0574	——	
1300 (2372)	3	1.3125	1.3045	0.0061	
1400 (2552)	3	1.5960	1.6041	0.0051	
1500 (2732)	3	1.9190	1.9304	0.0059	
1600 (2912)	3	2.2714	2.2802	0.0039	
1700 (3092)	——	——	——	0.005	EST.
1800 (3272)	——	——	——	0.005	EST.
1900 (3452)	——	——	——	0.005	EST.
PROCESSOR AT 75°C (167°F)					
600 (1112)	3	0.1544	0.1618	0.0476	
700 (1292)	3	0.2096	0.2126	——	
800 (1472)	3	0.3167	0.3094	——	
901 (1652)	3	0.4506	0.4401	——	
1000 (1832)	3	0.6156	0.6029	0.0207	
1100 (2012)	3	0.8254	0.8140	——	
1200 (2192)	3	1.0680	1.0574	0.0100	
1300 (2372)	3	1.2982	1.3045	——	
1400 (2552)	3	1.6103	1.6041	——	
1500 (2732)	3	1.9408	1.9304	——	
1600 (2912)	3	2.2885	2.2802	——	
PROCESSOR AT -55°C (-67°F)					
600 (1112)	3	0.1244	0.2126	N/A	
700 (1292)	3	0.2826	0.3094	N/A	
800 (1492)	3	0.4128	0.4401	N/A	
901 (1652)	3	0.5883	0.6029	N/A	
1100 (2012)	3	0.7953	0.8140	N/A	
1200 (2192)	3	1.0530	1.0574	N/A	
1300 (2372)	3	1.3596	1.3045	N/A	
1400 (2552)	3	1.6195	1.6041	N/A	
1500 (2732)	3	1.9660	1.9304	N/A	
1600 (2912)	3	2.3388	2.2802	N/A	

a. Ratio with maximum deviation from average at environmental temperature.

b. Calculated from the larger deviation of the 25 and 75°C (77 and 167°F) data sets.

Vibration A sinusoidal vibration survey scan was conducted while the output of the third-stage detector amplifiers were monitored (both silicon and germanium channels) with an oscilloscope. The first test was a sinusoidal sweep at .25 octive/min with a displacement of ±.064 mm (±.0025 in.) from 10 to 74 Hz and then an acceleration of 2 g's from 74 to 2000 Hz. The processor was vibrated on all three axes and no perturbations of the amplified optical signals were observed. The second test was conducted with the vibration perpendicular to the plane of the circuit board. The intensity of the vibrational excitation was increased to a displacement of ±.15 mm (±.006 in.) from 10 to 88 Hz and an acceleration of 5 g's from 88 to 2000 Hz. Again no perturbations could be detected on the oscilloscope and the performance factor for vibration was taken to be zero.

Comparison with Budget. The temperature deviations for the polynomial fit and environmental temperature of the processor are projected over the working temperature range of the sensor system in Fig 21. Twelve of the fifteen data points are near or below the budget value for that temperature. Three of the terms for the polynomial fit had significantly larger deviations. The larger error is believed to be due to the determination of the values, not the mathematical curve fitting procedure. Improvements in the measurement technique would, therefore, be expected to reduce the polynomial fit deviations.

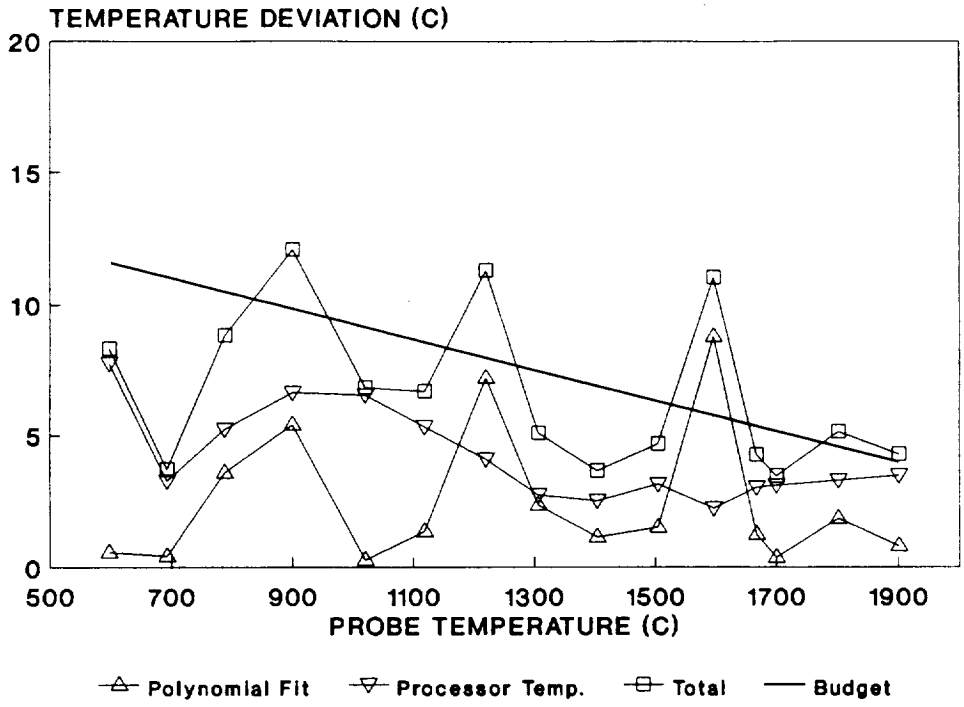

Figure 21. Reproducibility due to processor.

9.7 Sensor System Reproducibility

The factor affecting the reproducibility from the probe, cable and processor can be combined into a system reproducibility (see Figure 22). Nine of the fifteen data points are within the 14°C (25°F) budget and showed the

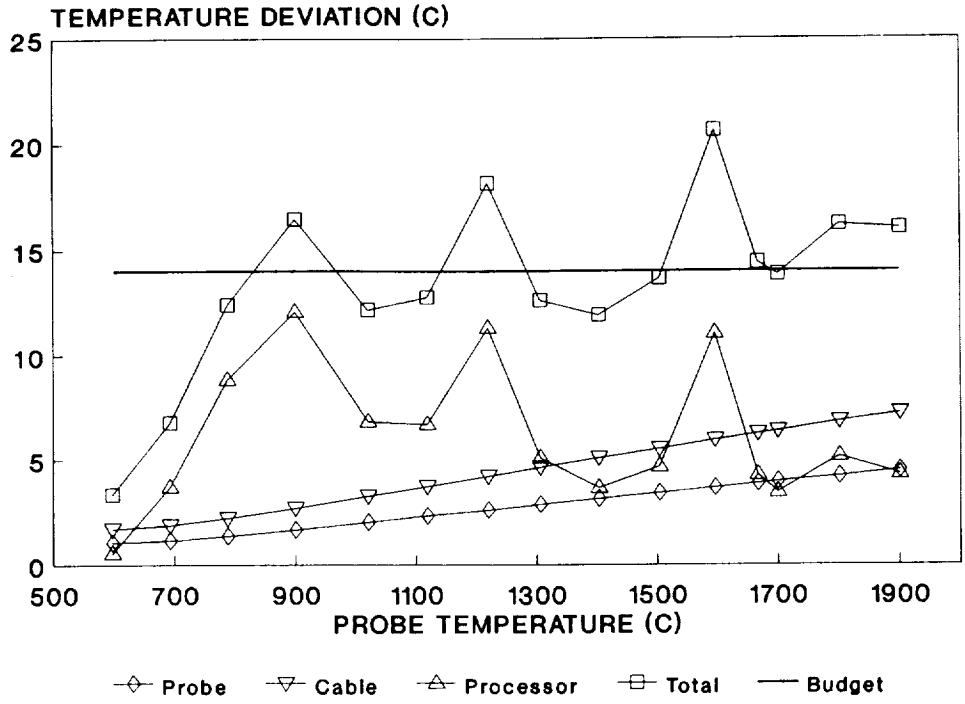

Figure 22. Reproducibility of Sensor System

potential of the system to make reproducible measurement over a wide range of environmental parameters. Improving the method of determining the polynomial data set is expected to bring the system reproducibility to within the budget value.

9.8 Reference Temperature

The reference temperature uncertainty reflects the difference in temperature in the polynomial data set and true temperature. The calibration procedure used to determine the polynomial data set was described in Section 7. Below 1700°C (3092°F) the polynomial data was determined experimentally. From 1700 to 1900°C (3092 to 3492°F) the theoretical dependence of intensity on temperature was used to extrapolate ratio versus temperature.

Temperature Uniformity. The temperature of the optical probe is assumed to be equal to that of the thermocouple located in the same calibration block. The probe and thermocouples are symmetrically located holes in the block, but their temperature may not be equal. A value of 2°C (3.6°F) was assigned as an uncertainty in the uniformity of the calibration fixture.

Thermocouple Uncertainty. The type B thermocouple used in these measurements was checked against a temperature standard calibrated by National Institute of Standard and Technology (see Table 18). The range of the comparison was constrained by the temperature limit of the furnace in the Calibration Laboratory at Conax Buffalo. Above 1200°C (2192°F) the thermocouple was assumed to be within 0.5% (Reference 28).

TABLE 18. REFERENCE TEMPERATURE

NOMINAL TEMP. °C (°F)	CALIBRATION LAB STD. UNCERTAINTY °C (°F)	THERMOCOUPLE B2 UNCERTAINTY[a] °C (°F)	COMBINED UNCERTAINTY °C (°F)
600 (1112)	0.6 (1.0)	2.9 (5.2)	3.5 (6.2)
700 (1292)	0.6 (1.0)	2.7 (4.9)	3.3 (5.9)
800 (1472)	0.6 (1.0)	2.5 (4.5)	3.1 (5.5)
900 (1652)	0.6 (1.0)	2.3 (4.1)	2.9 (5.1)
1000 (1832)	0.6 (1.0)	2.0 (3.6)	2.6 (4.6)
1100 (2012)	2.2 (1.0)	1.5 (2.7)	2.1 (3.7)
1200 (2192)	2.2 (4.0)	0.9 (1.6)	3.1 (5.6)
1300 (2372)	N/A	6.5 (11.7)	6.5 (11.7)
1400 (2551)	N/A	7.0 (12.6)	7.0 (12.6)
1500 (2732)	N/A	7.5 (13.5)	7.5 (13.5)
1600 (2912)	N/A	8.0 (14.4)	8.0 (14.4)
1700 (3092)	N/A	N/A	12.4 (22.3)[b]
1800 (3272)	N/A	N/A	19.2 (34.6)[b]
1900 (3452)	N/A	N/A	26.6 (47.9)[b]

a. Assumed to be 0.5% above 1200°C (2192°F)
b. Estimate from theory (see text)

Theoretical Extrapolation. The calibration block temperature was limited to below 1700°C (3092°F) by the available furnace. Higher temperatures could be created in flame but temperature control was inadequate for calibration purposes. As described in Section 9.1 the signal levels were found to follow the expected dependence on blackbody radiation. By baselining the theoretical ratio to the value measured at 1667°C (3033°F) the ratio could be extrapolated up to 1900°C (3452°F). The uncertainty in extrapolating to higher temperature was estimated by determining the departure of the theory from measured values at lower temperatures. These values are also listed in Table 18.

Combined Temperature Uncertainty. The uncertainty in the temperature used for the polynomial data set is plotted in Figure 23. The total value is greater than the budget of 5°C (9°F). At lower temperatures, using a thermocouple directly calibrated by National Institute of Standards and Technology (NIST) would reduce both the thermocouple uncertainty and the additive error of transferring temperature standards. NIST does not recommend using type B thermocouples above 1600°C (2912°F) and therefore use of the radiation theory will still be required. The large uncertainty in the theoretical extrapolation are due to simple nature of the theory. The theory uses the manufacturer's nominal responsitivities of the detectors. It is anticipated that measured responsitivities would greatly improve the accuracy of the extropolation.

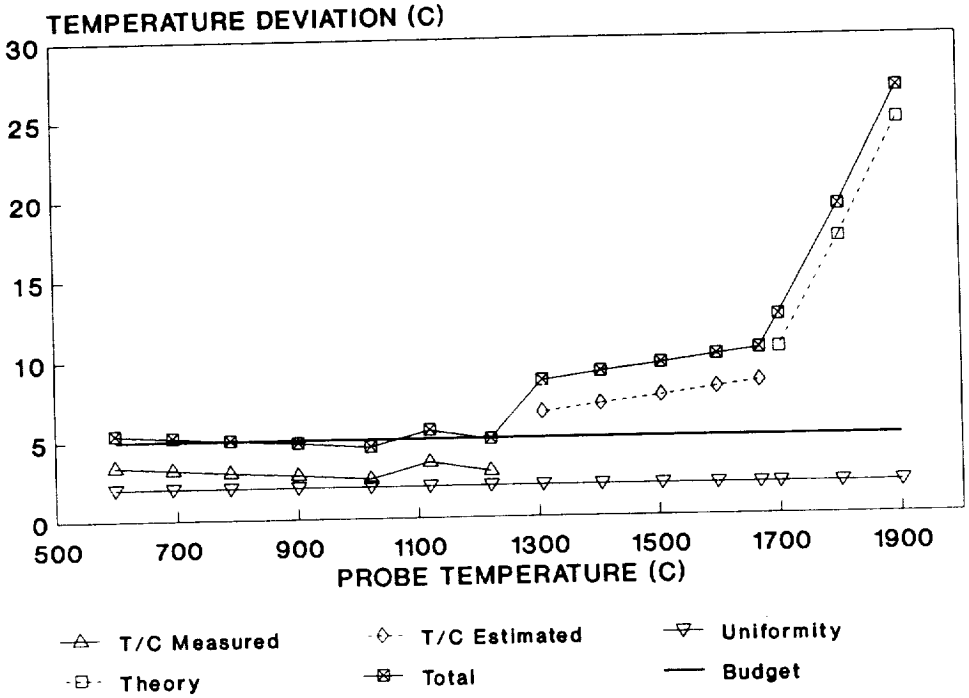

Figure 23. Uncertainty in reference temperature.

9.9 Sensor System Accuracy

The sensor system accuracy is simply the combination of the reproducibility of the system (specific combination a probe, cable and signal processor) and the uncertainty in the reference temperature. In Figure 24, these terms are compared to the goal of 19°C (34°F). Over most of the range the projected accuracy is better than 23°C (42°F) or 1.2% of full range. A more precise reference temperature standard would improve accuracy. Above 1600°C (2912°F) experimental calibration is limited by both furnace and thermocouple capability. Improvements in analytical prediction of probe signal ratio are required for this temperature regime.

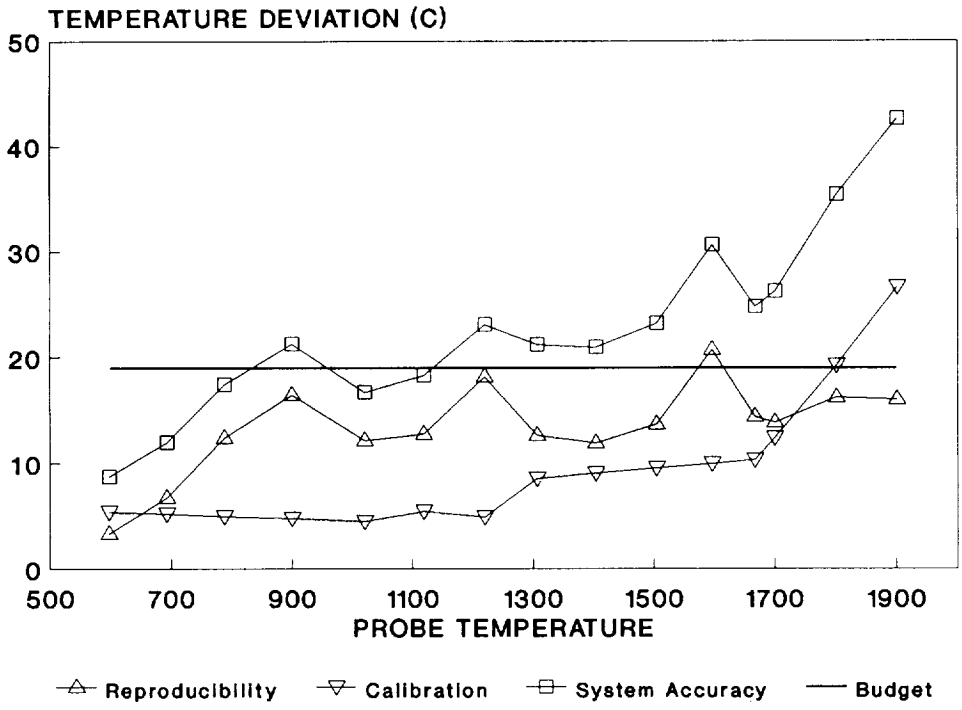

Figure 24. Sensor system accuracy.

10.0 TURBINE ENGINE TESTING

The first successful engine test of a fiber optic sensor conducted at General Electric Aircraft Engines Lynn, Massachusetts used the optical temperature sensor system shown in Figure 25. This system is based on technology developed under this contract and Conax Buffalo corporate funding. The fabrication and testing of four probes, the optical engine harness and jumper cables were paid for by General Electric.

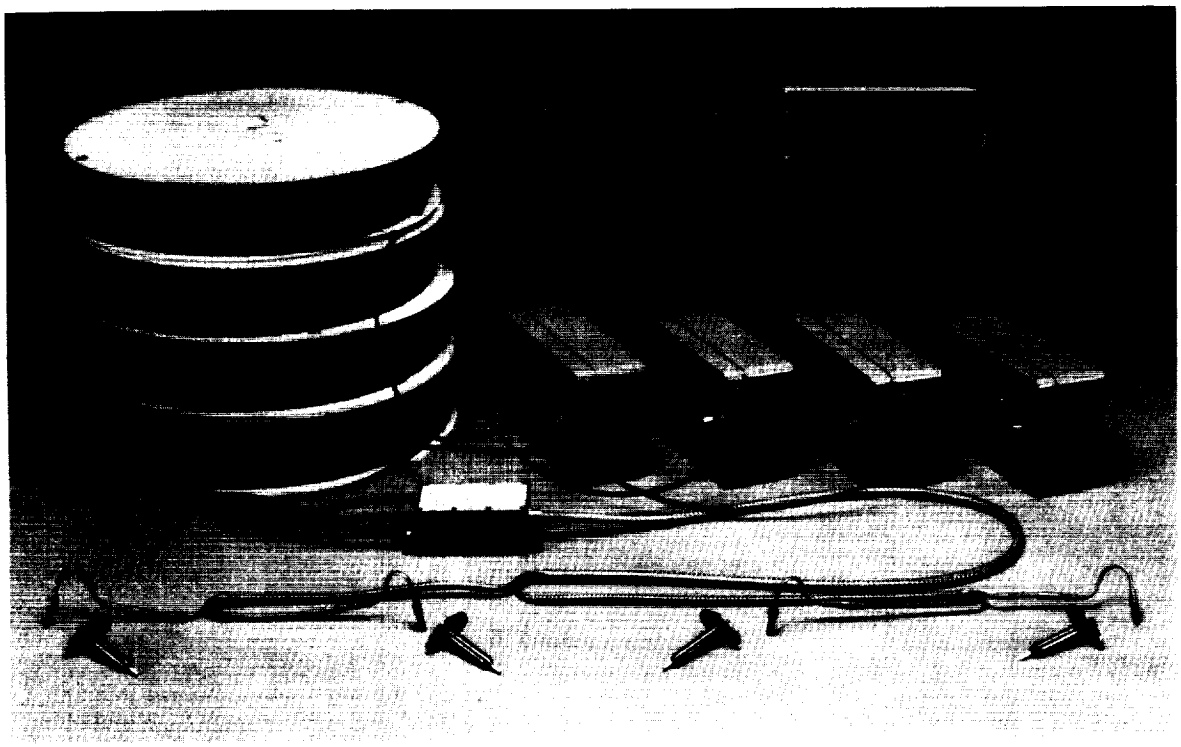

Figure 25. Turbine engine sensor system (shown with short probe housings but without sensing elements).

The optical sensor system was a functional equivalent to the four thermocouple probes used to measure gas temperature between the turbine and the afterburner (T5). Two of the probes had exposed sensing elements (open-end) and two longer probes (not shown in Figure 25) had shrouded sensing elements (closed-end). The four-fiber optical cable harness was mounted directly on the engine using the thermocouple harness brackets. Individual jumper cables allowed the four signal processors and display units to be located in the control room.

The optical system replaced the upper T5 half harness during an endurance test which started on January 9, 1990 and was completed on January 16, 1990. Significant results of the testing include:

- The system measured four temperatures in the pressurized turbine discharge region of the F404 turbine engine over the complete range of engine operating conditions.

- On-engine operation exceeded 50 hours, and an excess of 1000 thermal cycles were accumulated.

- The average temperatures measured by the individual fiber optic probes was in reasonable agreement with the average of the thermocouple probes.

- The open-end probes were still functional after the entire test sequence.

- The open-end probes responded faster than the average of the four thermocouple probes.

- The large afterburner flame, immediately downstream of the sensors, did not perturb the indicated temperatures with stray light.

- The probes and cables could be disconnected and reconnected with minimal affects on the indicated temperature.

- The probes and harness could be reinstalled, removed and reinstalled by engine technicians.

Most components of the optical T5 system performed throughout the test. Difficulties were, nevertheless, encountered with certain components.

- Contamination built up between the sapphire lightguide and optical connector. For the long probes, it degraded transmission after 30 hours so that the intensity was insufficient to pass the error checks in the signal processor.

- The vibration of the long probes caused one of the sapphire rods to brake, subsequent design changes were demonstrated to reduce resonance amplitude of the probe housing. The revised design has yet to be engine tested.

- The durability of the optical harness cable needs to be improved. One out of four joints failed between the fiber and connector after 45 hours.

The fact that the optical sensor system performed for an extended period on the F404 engine gives confidence in the basic design approach. No inherent barriers to the development of a production temperature sensor were identified.

11.0 CONCLUSIONS

A fiber optic sensor has successfully measured gas temperature in an aircraft turbine engine. The probe was designed specifically to withstand the severe environment in the high velocity engine flow. The sensing element used radiation from a thermally emissive insert in a sapphire rod. The sapphire rod acts as both a lightguide and shroud. The high melting point of sapphire allowed the probe to function at temperatures where exposed thermocouples would be destroyed. The small diameter of the sensing element provided a faster response time compared to conventional probes with metal shrouds. The signal processing used a ratio of optical intensity in two spectral bands and additional compensation to overcome the signal perturbation introduced by the engine environment.

A four probe system with an optical cable harness was tested as a functional replacement for the four thermocouples used to measure gas temperature between the turbine and the afterburner on a General Electric Aircraft Engines F404 engine. The duration of the engine test exceeded 50 hours and 1000 thermal cycles. The sensing elements with inserts were still functional after the test. Improvements in the durability of the components are needed for: 1. bonding the optical fiber to the connector since one of four cables failed after 45 hours, and 2. control of contamination that built up at the interface between the sapphire rod and the connector. No inherent limitations to the use of this fiber optic temperature sensor were identified during the test.

The sensing element has been demonstrated to function in a high temperature combustion environment. Sensing elements were tested in a propane flame to 1931°C (3508°F) at low velocity and up to 1500°C (2732°F) at Mach .37. Other environmental effects such as vibration and stray light from the afterburner can be accounted for with proper probe design.

The response time was observed to be faster than the thermocouple probes used to measure turbine exhaust temperature. A measured time constant of 1 second at one atmosphere was projected to reduce to .28 seconds at an advanced turbine mass flux of 1000 kg m^{-2} s^{-1} (205 lb ft^{-2} s^{-1}). The response time could be reduced with a smaller diameter sapphire rod, however, for the current sensing element length, an undesirable resonance frequency would result.

An optical cable harness was successfully designed and tested for the 260°C (500°F) temperature and $\pm$0.64mm ($\pm$0.025 in) vibrational displacement encountered on a turbine engine. Performance testing showed that using a signal ratio provides the necessary correction for intensity perturbations caused by connector remating, cable bending, ambient temperature changes and vibration. Cable bending was identified as the dominant error source, and, as such, the cable bend radius must be kept greater than 100 mm (4 in).

Conax Buffalo had developed the essential signal processing electronics prior to the start of this Phase II Program. The Conax design was adapted to meet specific program requirements of: a single circuit board, wider environmental and measurement temperature range, operation on 28 VDC, a ruggedized housing, and expanded built-in-test features. All the necessary functions to accept an optical signal from the probe and produce a digital value of the temperature were packaged in a enclosure with dimensions of 220 x 120 x 85 mm (8.66 x 4.72 x 3.35 in). The optical and electrical interface was provided through a single, military-style circular connector.

The signal processor was demonstrated to be suitable for on-engine operation by functioning over a temperature range of -55 to 75°C (-67 to 167°F) and at vibration level of 2 g's. The environmental temperature perturbed the signal level by as much as 38%, but the microprocessor based system was programmed to compensate for these effects. The deviation of the indicated probe temperature was limited to between 2 and 8°C (3.6 and 14°F) over the environmental range of the processor from 25 to 75°C (77 to 167°F).

The system accuracy was defined to be the combination of reproducibility and the calibration reference temperature. Reproducibility reflected the variation of the indicated temperature with multiple readings or deviations caused by environmental effects. The system was projected to be within the reproducibility budget of 14 °C (25°F) over most of the measurement range. Calibration required that the sensing element be located in a reference temperature zone which can be related to true temperature. Up to 1200°C (2192°F) it was estimated that the reference temperature was known within 5.7°C (10.3°F) of true temperature. Limits on present equipment precluded direct assessment at higher temperatures and consequently the uncertainty increased. The technology exists to improve the determination at the higher temperature, but it was not possible to implement these changes within the program time frame.

The technology developed in this program extends the range of gas temperature measurement in turbine engines. Present combustors exceed the 1788°C (3250°F) limit of platinum based thermocouples for ground test instrumentation. Durability considerations for production engine sensors limit their range to below 1200°C (2192°F). Thus, the 1900°C (3452°F) capability of the fiber optic sensor offers advantages in both applications. The optical probe operation was not characterized above 1900°C (3452°F) and, if future combustion systems exceed this value, additional research would be required.

The use of a fiber optic temperature sensor on a production engine would make durability and weight primary design considerations. Direct measurement of turbine inlet temperature would be difficult to achieve with a low weight housing. For the next generation engine design, it is recommended that the temperature sensor be incorporated into the structure of the first or second turbine vane. This location would reduce the present extrapolation of downstream measurements to provide a limit on upstream hardware temperatures.

In summary, the Phase II Program met the objective of demonstrating the ability of a fiber optic temperature sensor to operate on an aircraft turbine engine. Further, the sensing element operated at temperatures up to 1900°C (3452°F) which cannot be obtained with exposed thermocouple probes. Optical cables and a compact signal processor have also been demonstrated to be suitable for on-engine operation.

APPENDIX A
SENSOR QUALIFICATION REQUIREMENTS

Environmental temperature and vibration are key specifications for the sensor. The temperature range for the probe, cable, and processor would not be controlled with MIL-STD-810C because of the unique requirement of an individual engine. The engine manufacturer would control the temperature requirement with a company written specification. The vibration would probably use the procedures called out in MIL-STD-810C but modify the vibration spectrum to an engine specific envelope.

All engine sensor hardware would be subjected to an extensive series of qualification tests. While most of these tests would not necessarily be required for ground tests, the design should anticipate the requirements for flight hardware. Tables 19 to 21 list the requirements known at this time.

TABLE 19. ANTICIPATED SPECIFICATIONS FOR PROBE

Parameter	Specification
Operating Temperature	Engine Manufacturers Specification
Storage Temperature	MIL-STD-810C high, Section 501.2 Procedure I. low, Section 502.2, Procedure I.
Temperature Shock	MIL-STD-810D, Section 503.2
Vibrations	MIL-STD-810D, Section 514.3 with spectrum specified by engine manufacturer
Acoustic Noise	MIL-STD-810D, Section 515.3
Acceleration	MIL-STD-810D, Section 513.3
Shock	MIL-STD-810D, Section 616.3
Altitude	MIL-STD-810D, Section 500.2
Humidity	MIL-STD-810D, Section 507.2
Sand and Dust	MIL-STD-810D, Section 510.2
Salt Fog	MIL-STD-810D,Section 509.2
Fungus	MIL-STD-810, Section 508.3
Connector mating	MIL-STD-1344A
Cable Seal/Strain Relief	MIL-STD-1344A
Compatibility	Materials: Jet Fuel Lubricating oil Ethylene Glycol Isopropyl Alcohol

TABLE 20. ANTICIPATED SPECIFICATIONS FOR CABLE AND CONNECTOR

Parameter	Specification
Connector Geometry	MIL-C-83522A
Operating Temperature	Engine Manufacturers Specification
Storage Temperature	MIL-STD-810C high, Section 501.2 Procedure I. low, Section 502.2, Procedure I.
Temperature Shock	MIL-STD-810D, Section 503.2
Temperature Cycling	MIL-STD-1344A, Method 1003
Vibrations	MIL-STD-810D, Section 514.3 with spectrum specified by engine manufacturer MIL-STD-1344A, Method 2005
Acoustic Noise	MIL-STD-810D, Section 515.3
Acceleration	MIL-STD-810D, Section 513.3
Shock	MIL-STD-810D, Section 616.3 MIL-STD-1344A, Method 2004
Altitude	MIL-STD-810D, Section 500.2
Humidity	MIL-STD-810D, Section 507.2 MIL-STD-1344A, Method 1002A
Sand and Dust	MIL-STD-810D, Section 510.2
Salt Fog	MIL-STD-810D,Section 509.2 MIL-STD-202E, Method 110A
Fungus	MIL-STD-810, Section 508.3
Mating Durability	MIL-STD-1344A, Method 2016
Cable Seal/Strain Relief	MIL-STD-1344A, Method 2017
Cable Retention	MIL-STD-1344A, Method 2009
Compatibility	Materials: Jet Fuel Lubricating oil Ethylene Glycol Isopropyl Alcohol Hydraulic Fluid

TABLE 21. ANTICIPATED SPECIFICATIONS FOR SIGNAL PROCESSOR

Parameter	Specification
Operating Temperature	Engine Manufacturers Specification
Storage Temperature	MIL-STD-810C high, Section 501.2 Procedure I. low, Section 502.2, Procedure I.
Temperature Shock	MIL-STD-810D, Section 503.2 or MIL-STD-202, Method 107
Vibrations	MIL-STD-810D, Section 514.3 or MIL-STD-202 Method 204 with spectrum specified by engine manufacturer
Acoustic Noise	MIL-STD-810D, Section 515.3
Acceleration	MIL-STD-810D, Section 513.3
Shock	MIL-STD-810D, Section 616.3 or MIL-STD-202, Method 213
Altitude	MIL-STD-810D, Section 500.2
Humidity	MIL-STD-810D, Section 507.2 or MIL-STD-202, Method 106
Electronic Interference	MIL-STD-461B, MIL-STD-462, MIL-HNBK-235-1
Lightning Protection	Tested as part of engine control

REFERENCES

1. Bird, V., Sweeney, P., and Kirby, P., "Fiber-Optic Turbine Inlet Temperature Measurements System (FOTITMS)," Allison Gas Turbines and Land Infrared, Paper AIAA 90-2033, Presented at the AIAA/SAE/ASME/ASEE 26 Joint Propulsion Conference, Orlando FL, July 16-18, 1990.

2. Smith, C. J., "The Promise of Advanced Materials for a 21st Century UBE," General Electric Aircraft Engines, AIAA Paper 90-2396, Presented at the AIAA/SAE/ASME/ASEE 26 Joint Propulsion Conference, Orlando FL, July 16-18, 1990.

3. Burcham, F., Gilyard, G., and Myers, L., "Propulsion System - Flight Control Integration - Flight Evaluation and Technology Transition," NASA Ames Research Center, Dryden Flight Research Facility, AIAA Paper 90-2280, Presented at the AIAA/SAE/ASME/ASEE 26 Joint Propulsion Conference, Orlando FL, July 16-18, 1990.

4. Skira, C. and Agnello, M., "Aircraft Propulsion Control Systems for the Next Century," Wright-Patterson AFB and Naval Air Propulsion Center, AIAA Paper 90-2034, Presented at the AIAA/SAE/ASME/ASEE 26 Joint Propulsion Conference, Orlando FL, July 16-18, 1990.

5. Baumbick, R. J., "Fiber Optics for Advanced Aircraft," Fiber Optics and Laser Sensor IV, SPIE Vol. 985, 1988, pp. 5-11.

6. Poppel, G. L., Glasheen, W. M., and Russell, J. C., "Fiber Optic Control System Integration," General Electric Aircraft Engines, NASA CR-179568, Feb. 1987.

7. Poumakis, D. J., and Davies, W. J., "Fiber Optic Control System Integration," Pratt & Whitney, NASA CR-179569, Dec. 1986.

8. Poppel, G. L., and W. M. Glasheen, "Electro-Optic Architecture for Servicing Sensors and Acturators in Advanced Aircraft Propulsion Systems," General Electric Aircraft Engines, NASA CR-182269, June 1989.

9. Glomb, Jr., W. L., "Electro-Optic Architecture (EOA) for Sensors and Acturators in Aircraft Propulsion Systems," United Technology Research Center, NASA CR-182270, June 1989.

10. Nitka, II, E. F., "Application of Fiber Optic Sensors in Advance Engine Controls," Fiber Optics and Laser Sensor IV, SPIE Vol. 985, 1988.

11. Davidson, I. "The Use of Optical Sensors and Signal Processing in Gas Turbine Engines," Rolls-Royce, Paper 1374-27, Presented at SPIE Conf. EO/Fibers '90, Sept 16-21, San Jose, CA.

12. Stewart, J. E., Evans, D. E., and Larson, G. L. "Remote Radiation Temperature Sensor," U.S. Patent 3,626,758, Dec. 14, 1971.

13. Dils, R. R., "Optical Fiber Thermometer," U.S. Patent 4,576,486, March 18, 1986.

14. Dils, R. R., "High Temperature Optical Fiber Thermometer," J. of Applied Physics, Vol. 54 1983, pp. 1198-1201.

15. Mossey, P. W., Shaffernocker, W. M., and Mulukutla, A. R., "1700°C Optical Temperature Sensor," General Electric Aircraft Engines, NASA CR-175108, July 1986.

16. Swithenband, J., "Advanced Instrumentation for Aeroengine Components," In AGARD Conference Proceedings, No. 399, 1986.

17. Tregay, G. W., "Optical Fiber Temperature Sensor," U.S. Patent 4,794,619, Dec. 27, 1988.

18. Mattingly, J. D., Heiser, W. H., and Daley, D. H., Aircraft Engine Design, American Insititute of Aeronautics and Astronautics, New York, NY, 1987 pp. 295-330.

19. Powel, IV, S. F., "On the Leading Edge: Combining Maturity and Advanced Technology on the F404 Turbofan Engine," Paper 90-GT-149, Presented at the Gas Turbine Congress and Exposition, June 11-14, Brussels, Belgium.

20. Dix, D. M., and Petty, J. S., "Aircraft Engine Technology Gets a Second Wind," Aerospace America, July 1990, pp. 36-39.

21. Scadron, M. D., Warshawsky, I., and Gettelman, C., "Thermocouples for Jet-Engine Gas Temperature Measurement," ISA Proceedings, Vol. 7, 1952 pp. 142-154.

22. Williamson, R. C., and C. M. Stanforth, "Measurement of Jet Engine Combustion Temperature by the Use of Thermocouples and Gas Analysis," Paper 690433, Presented at the SAE National Air Transportion Meeting, New York, NY, April 21-24, 1969.

23. The Preparation and Use of Chromel-Alumel Thermocouples for Aircraft Gas Turbine Engines, SAE Report AIR 46 Rev. A. Jan. 1990.

24. Ryshewitch, E. and Richerson D. W., Oxide Ceramics, Academic Press, Inc., Orlando, FL, 1985, pp 177-205.

25. Holman, J. P., Heat Transfer, McGraw-Hill Book Co., New York, 1976, pp 212-220, p. 503.

26. Glomb, Jr., W. L., "Fly-by-light Schemes Move into Demonstration Stage," Laser Focus World, Vol. 26, Number 6, June 1990, pp. 167-176.

27. Scadron, M. D. and Warshansky, I., "Experimental Determination of Time Constant and Nusselt Numbers for Bare-Wire Thermosouples in High Velocity Air Streams and Analytic Approximation of Conduction and RAdiation Errors," National Advisory Committee for Aeronautics, Technical Note 2599, June 1952.

28 Powell, R.L., Hall, W.J., Hyink, Jr., C., Sparks, L.L., Burns, G.W., Scroger, M.G., and Plumb, M.M., "Thermocouple Reference Tables Based on IPTS-68," National Bureau of Standards Report COM-74-50351, March 1974, pp. 47-51.